Synsint Research Group

Available online at www.synsint.com

Synthesis and Sintering

ISSN 2564-0186 (Print), **ISSN** 2564-0194 (Online)

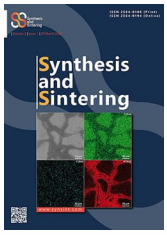

Review article

Recent advances in hydrogen production using MXenes-based metal sulfide photocatalysts

Asieh Akhoondi [a,*], **Hadi Ghaebi** [b], **Lakshmanan Karuppasamy** [c], **Mohammed M. Rahman** [d,*], **Panneerselvam Sathishkumar** [e]

[a] *Department of Chemical Engineering, Arak Branch, Islamic Azad University, Arak, Iran*
[b] *Department of Mechanical Engineering, Faculty of Engineering, University of Mohaghegh Ardabili, P.O. Box 179, Ardabil, Iran*
[c] *Department of Environmental Engineering and Science, Feng Chia University, Taichung 407, Taiwan*
[d] *Department of Chemistry, King Abdulaziz University, Jeddah 21589, P.O. Box 80203, Saudi Arabia*
[e] *Department of Chemistry, School of Advanced Sciences, Vellore Institute of Technology (VIT), Vellore - 63014, India*

A B S T R A C T

At present, the composition and crystalline structure of transition metal nitrides or carbides (MXenes) and their derivatives are continuously expanding due to their unique physicochemical properties, especially in the photocatalytic field. Advances over the past four years have led to improved preparation of new MAX phases, resulting in new MXenes with excellent photo-thermal effect, considerable specific surface area, long-term stability and optimum activity. Since MXenes have good electrical conductivity and their bandgap is adjustable under the visible light range, this group is one of the best promising candidates for hydrogen production from photo-splitting of water as an environment-friendly method of converting sunlight to chemical energy. Progress in noble metal-free photocatalyst associated with more understanding of the fundamental mechanism of photocatalysis has enabled a proper choice of cocatalyst with better efficiency. In this study, the photocatalytic production of hydrogen through MXens as a support and co-catalyst on metal sulfide is summarized and discussed. Recent advances in the design and synthesis of MXenes-based metal sulfide nanocomposites to increase the efficiency of photocatalytic hydrogen production are then highlighted. Finally, the challenges and future prospects for the development of MXenes-based metal sulfide composites are outlined.

KEYWORDS

MXenes-based metal sulfide
Photocatalyst
H_2 production
Semiconductor
Synthesis

OPEN ACCESS

1. Introduction

In the present century, the energy crisis is one of the problems of advanced and developing societies, which has caused many researchers to focus on energy storage. Because the world's need for energy is growing and environmental pollution is having a devastating effect on human life, sustainable and renewable energy sources, such as solar energy, could potentially replace fossil fuels and reduce CO_2 emission [1]. To solve the environmental problems and growing energy crisis, photo-evolutionary hydrogen is a new and appropriate solution that has undergone extensive research. In the last three decades, advances have been made in photocatalysts and the absorption of visible light to convert solar energy directly into chemical energy [2]. One of the applications of semiconductor photocatalysts is the production of hydrogen through the water-split reaction [3]. Other applications include air purification [4] and water treatment through decomposition

* Corresponding author. *E-mail address:* asieh.akhoondi@gmail.com (A. Akhoondi), mmrahman@kau.edu.sa (M.R. Rahman)
Received 27 February 2022; Received in revised form 28 March 2022; Accepted 29 March 2022.

https://doi.org/10.53063/synsint.2022.21106

of pollutants [5], nitrogen fixation [6], carbon dioxide conversion [7], H_2O_2 production [8] and more. Photocatalysts have unique properties, including good optical bandgap, thermal and chemical stability, and non-toxicity, which are made from high-permeability elements in earth crust [9].

In the last decades, photocatalysts as photo-reaction accelerators have been utilized in a large variety of chemical reactions. Therefore, in photocatalytic processes, reactions are carried out by a semiconductor as a catalyst (light absorber) that changes the rate of a chemical reaction under irradiation of ultraviolet and visible light range. In photocatalytic process, the main factor in light harvesting and conducting the reaction progress are photocatalysts. Hence, the use of photocatalysts in solar energetic replacement technologies is undeniable for environmental green process. Many semiconductors with oxide, sulfide, nitride and phosphate compounds, etc. have been investigated under visible light [10–13]. Because single photocatalysts do not perform effectively due to the rapid recombination of charge carriers and their low quantum efficiency, different co-catalysts with different structures are used [14]. Strategies such as elemental doping, surface sensitization, unstructured production and facet control lead to improved charge carrier separation [15–18].

The MAX phase family, which is mainly intermediate metal carbides, can be peeled into two dimensions known as MXenes. Max phases are layered solids with the general formula $M_{n+1}X_nT_y$ shown that "M" is an intermediate metal (mostly groups 4 and 5 of periodic table including Ti, Zr, V, Nb, Cr and Mo) with values n = 1, 2, 3, "X" is carbon and/or nitrogen and "T" is a surface functional group such as OH, O, Cl, and F [19, 20]. MXenes are constructed through a selective etching of the early transition metal layer (groups 12 and 14 of the periodic table) of the MAX phase, as shown in Fig. 1. The promising features of MXenes, including oxidation resistance, adjustable structure, high surface area, hydrophilicity, high conductivity, and earth-abundant, cause to attract much attention in the photocatalysis field [21]. Furthermore, the silylation reagents introduce adjustable hydrophilicity to MXene [22]. Ti_3C_2 MXene was one of the first MXenes to undergo chemical etching, and later MXene variants were made using various methods [23]. Other MXenes such as $Ti_xTa_{(4-x)}C_3$ [24], Nb_2CT_x [25], Mo_2CT_x [26], Mo_2TiC_2 [27] and Nb_2C [28] are promising candidate for Li batteries and photocatalytic process. Also Nb_2C has been used in photospltting of water [29] and photocatalytic degradation of organic pollutants [30]. It has been shown that MXenes can undergo an electronic transition from metal properties to semiconductors due to the electronegativity of transition metals after functionalization [19].

The special structure, superior photochemical properties and sufficient metallic conductivity, provided by $Ti_3C_2T_x$ make it a very desirable auxiliary semiconductor for H_2 production compared to non-commercial catalysts [31]. MXenes can participate in photocatalytic processes as co-catalysts alongside semiconductors due to low Fermi level of these solid compounds. In order to photoelectrocatalytic and photocatalytic water splitting, research developed on MXene materials as two dimensional semiconductor-mediated photocatalysts [32, 33]. The most famous MXene (among more than 70 fabricated MAX phases) is Ti_3C_2, which is used in the production of hydrogen along with semiconductors such as g-C_3N_4 [34] WO_3 [35] and Ag_2S [36] to take entire advantages of MXene hybrids. Meanwhile, MXene/TiO_2 based nanocomposite is the most extensively used MXene system for hydrogen generation under the visible light spectrum [37]. Additionally, $Ti_3C_2T_x$ as a 2D transition metal carbide material is one of the best co-catalyst for H_2 generation from water splitting reaction, because of its tunable bandgap and high electronic conductivity [38]. Besides, high specific surface area, exposed metallic active sites and tunable terminal functional groups (−F, −O, and −OH) distinguish $Ti_3C_2T_x$ from other co-catalysts. Nevertheless, low photocatalytic activity is a major challenge which restricts the use of photocatalysts [39]. Therefore, Mxenes are combined with other semiconductors to improve the separation of charge carriers and enhanced catalytic activity beyond the individual MXene [40, 41]. The most stable Mxenes 2D mode belongs to OH*/O*-terminated Mxenes that take good charge transfer [42]. In two-dimensional Mxenes, oxygen surface atoms act as catalytic activated sites in the reaction of hydrogen evolution, which has compatible interaction potency with H* and by combining a suitable semiconductor, they can have high performance in solar driven hydrogen generation for energy storage. Although extensive research has been made about 2D semiconductor photocatalysts, there are still great challenges to overcome their destruction, charge transfer along with recycling and low-cost efficiency, which inhibits commercial-scale application extremely [43]. Nanoscale metal sulfides and transition metal chalcogenides have many

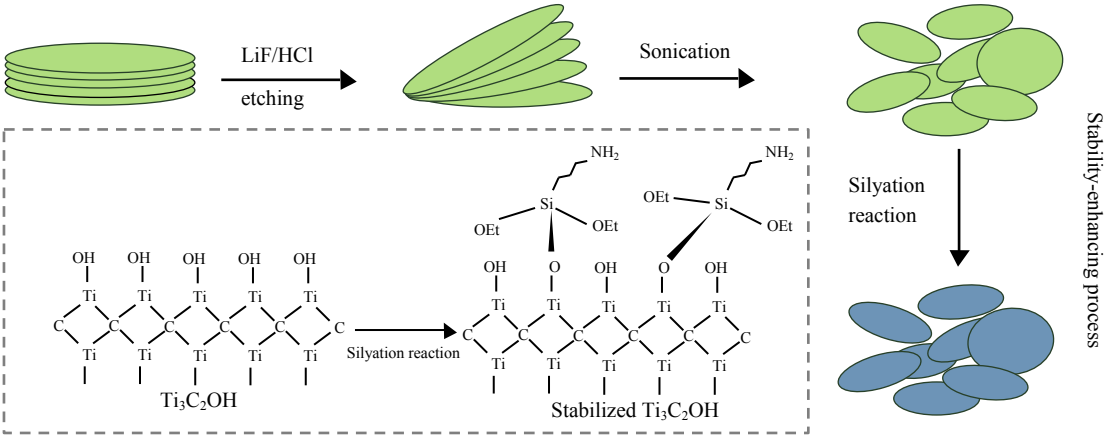

Fig. 1. Schematics of the Mxenes development from the MAX phase through the selective etching layer A and applying sound energy.

applications in optoelectronic and electronic devices, solar cells, batteries and photocatalysis due to their excellent properties and coordinated arrays in the infrastructure [44]. The general easy synthesis procedure, abundance, and low cost of these groups such as FeS_2 [45], Cu_2S, [46] , In_2S_3, [47] and Ni_3S_2 [48] cause to have attracted much attention in the field of energy storage [49]. Although these materials have a high quantum yield and short charge transfer distance, they have little efficiency in photocatalytic reactions because they are severely unstable under long-time solar-simulated radiation [50]. Among all semiconductors with different dimensions, zero-dimensional transition metal chalcogenides such as quantum dots, especially metal sulfide (MSs: ZnS, MoS_2, etc.), have attracted a lot of consideration due to integrated structural benefits which include: i) numerous active sites; ii) shorter distance of charge transfer ; iii) great light absorption in the visible or near-infrared area iv) adjustable bandgap and emission of many e^- from the valence band to the conduction band per absorbed photon [51]. However, quantum dots on nanostructure of metal sulfides and metal chalcogenides cause the effects of a strong optical edge, which makes it possible to use them under the visible light spectrum. For the synthesis of these materials, various methods such as surface modification, microwave-assisted solvothermal, precipitation, ion-exchange, hydrothermal method and ultrasonic chemical method are used to be explained below [52, 53].

Metal sulfides semiconductors are a potentially important class of abundant, non-toxic earth materials used to convert solar energy into chemical energy. Pairing MXens and metal sulfides with appropriate bandgap is a promising approach to increase light absorption and charge separation. Previously there have already been several reports of MXene-based composites on the water splitting with solar energy, but there is no single study on metal sulfide development with current advances in the field. In this review, we study the composite formation and describe the photocatalysis structure and properties of MXenes towards the photocatalytic hydrogen generation. Firstly, the foundations of photocatalytic processes, steps and requirements are explained. Secondly, artificial synthesis methods of metal sulfides have been discussed, followed by metal sulfide-based photocatalysts on MXenes specially Ti_3C_2. Subsequently, the widespread aspects of the applications of Mxene/metal sulfide nano hybrids are emphasized by the environmental and energy production approach, under visible and invisible light illumination. Finally, a summary of the future perspective has been raised from deep communication and understanding of this issue. In addition, the comprehensive overview of the Mxene/metal sulfide in the field of hydrogen evolution is presented under various conditions to design an efficient photocatalyst for overcoming the energy problem.

2. The general principles of photocatalysis

A phenomenon in which a semiconductor exposed to light produces electron/hole (e^-/h^+) pairs is called photocatalysis. The desired products are generated with the participation of both electrons and holes under a redox reaction [54]. In photocatalytic processes, light energy is utilized to absorb photon at first, then produce electron/hole pairs, separate charge carriers and so chemical reaction occurs then charges recombine. When the excited electrons lose their energy by releasing unproductive heat, they combine with the holes again. Semiconductors as photocatalytic materials should have properties such as: 1) suitable bandgap for absorbing visible light with sufficient optical edge potential, 2) ability to separate excited electron/holes pairs produced by photons, 3) chemical stability against photo-corrosion, 4) minimize energy losses during charge transfer and electron/hole recombination, and 5) low production costs.

Some active groups such as superoxide radical ($^{\bullet}O^{2-}$), hole (h^+) and hydroxyl radical ($^{\bullet}OH$), participate in reactions [55]. The basic mechanism in photocatalytic processes consists of three stages: production of electron/holes pairs (redox centers), interfacial electron transfer from and to substrates (often coupled with proton-transfer), and conversion of primary redox intermediates into the products [50]. At the beginning of the process in the valence band (VB) with the impact of light, an electron/hole pair is produced. Radiation hitting the surface of the photocatalyst must have enough energy (greater than or equal to the bandgap energy) to produce an electron/hole pairs. The electrons are then separated from the holes in the VB and migrate to conduction band and excited in the CB [56]. Factors restrict the photocatalytic activity of semiconductors, such as the low number of reactive sites on the surface, the rapid recombination of electron/hole pairs. Fig. 2 shows several types of single semiconductors with their bandgaps. As shown in this figure, molybdenum sulfide has a relatively weak bandgap for absorbing visible light illumination. So, it is strongly recommended that the MoS_2 be modified with CdS or $ZnIn_2S_4$ by

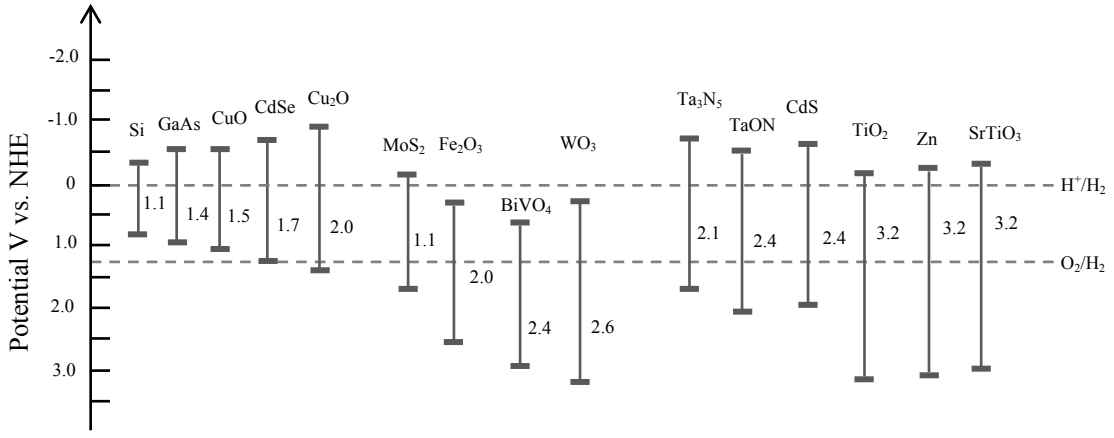

Fig. 2. Band potentials of various photocatalyst materials showing band positions and bandgaps for possible hydrogen evolution in photocatalysts.

introducing additional components to improve photo-absorption ability [57]. However, all three MoS_2, CdS and $ZnIn_2S_4$ have a crucial drawback due to their photocorrosive character. Sulfur ions in these semiconductors are oxidized by h^+ produced by light instead of water, while metal ions are dissolved in water [58]. MXenes have large surface area that prevent the accumulation of metal sulfide and increase the efficiency of photocatalysis. The large surface area of MXene can reduce metal sulfide agglomeration and enhance the photocatalytic effect. In addition, titanium has a strong redox reaction on the MXenes surface, so that the whole photocatalytic system has a stronger oxidation and reduction ability, thus the goal of enhancing the photocatalytic efficiency is achieved [36].

2.1. Role of MXenes in H_2 evolution

MXenes as a support material with hydrophilic surface for hybridization with other semiconductors have excellent H_2 evolution activities. Among the MXenes family, $Ti_3C_2T_x$ differs greatly in chemical properties from other members of this class because it has abnormal surface end groups. The role of $Ti_3C_2T_x$ with a high specific surface as co-catalyst in MXene/metal sulfide nanocomposite is to create active sites and terminals at the oxygen surface that act as charge separators for H_2 generation from water splitting reaction. Hence, MXene plays an important role in increasing the efficiency charge separation and transfer by modulating the migration of electrons from quantum surfaces [59]. Moreover, hydrogen bonding and electrostatic interaction between contacted MXene and metal sulfide can improve the stability of the photocatalyst [36].

The mechanism of the photocatalytic reaction of water splitting involves the reaction of producing hydrogen and oxygen. The impact of the light beam on the surface of the photocatalyst stimulates the metal sulfide and leads to the formation of electron/hole pairs. At pH 7, the initial transfer of e^- to the H^+ ion takes place to produce hydrogen, which occurs energetically in the visible region of light. The negative Fermi level is provided by the ohmic contact between MXene and metal sulfide, which causes accumulation of electrons on the surface of co-catalyst and convert H^+ to H_2. Moreover, the electron donor or scavenger reduces the remaining holes in the valence band of semiconductor. In general, photosplitting of H_2O involves some fundamental steps such as photon-absorptions, separation of e^-/H^+ pairs, influence and transfer of charge carriers, and the final function of catalyst. Applications of co-catalyst and donor factors that are organic solvents prevent the recombination of the electron/hole and suppress the recombination with the consumption of h^+. The steps for hydrogen generation from water splitting reaction are as follows:

$$\text{Catalyst} + h\upsilon \rightarrow e^- + h^+ \quad (1)$$

$$2H_2O + 4h^+ \rightarrow O_2 + 4H^+ \text{ (oxidation reaction)} \quad (2)$$

$$2H^+ + 2e^- \rightarrow H_2 \text{ (reduction reaction)} \quad (3)$$

$$H_2O + h\upsilon \rightarrow H_2 + 1/2O_2 \text{ (overall reaction)} \quad (4)$$

In general, the number of active sites enhances with increasing specific surface area. The amount of holes sacrifice and electron/hole pair separation depends on the number of active sites. Therefore, the use of donors will help improve the photocatalytic process and have a new perspective of photocatalytic parameters. Sacrificial agents not only play the role of electron donor but also reduce the charge carriers' recombination rate. Fig. 3 shows the mechanistic route for effective charge separation in Ti_3C_2-based/metal sulfide in hydrogen evolution under sunlight illumination. Theoretically, semiconductors having a minimum bandgap of 1.23 eV (redox potential) are suitable for efficient photocatalytic H_2 evolution to reduce resistances of photo-generated e^- and h^+ through charge transfers and desired reactions.

2.2. Role of sacrificial agent

The photocatalytic reaction of water splitting for hydrogen evolution is heavily dependent on sacrificial agent. Sacrificial agents or electron donors/hole scavengers play a prominent role next to the selected photocatalyst. In the case of sulfide catalysts, sulfide/sulfite-based sacrificial factors can quickly be absorbed on the photocatalyst surface and absorb h^+ in comparison with glucose and alcoholic matter such as methanol, ethanol, and isopropanol [60]. The alkaline environment derived from sulfide and sulfate solutions or amine compounds for hydrogen generation is preferable to glucose and alcohol that produces

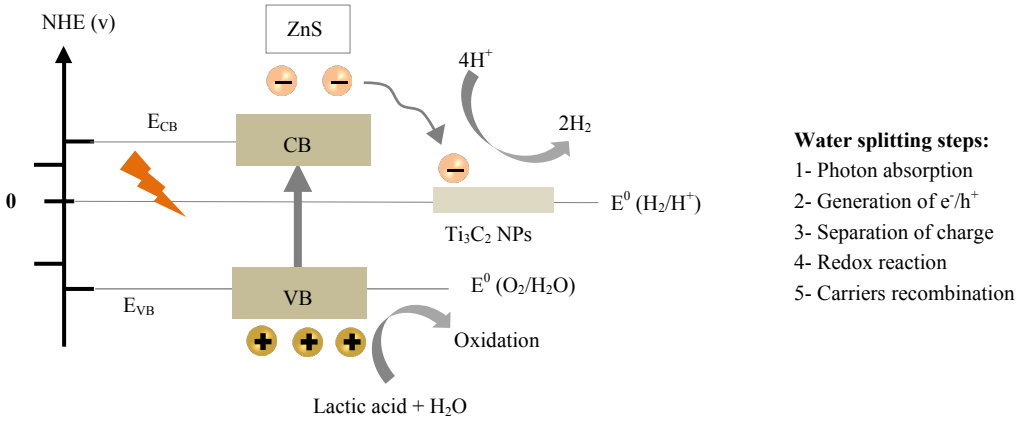

Fig. 3. Mechanistic route for effective charge separation in Ti_3C_2 co-catalyst and metal sulfide and the corresponding photocatalytic H_2 production under visible light irradiation.

a solution with neutral pH. The utillizing of Na_2S, Na_2SO_3, Na_2S/Na_2SO_3, triethanolamine (TEOA) and lactic acid as sacrificial factors leads to the photogeneration of hydrogen [61]. Biomass glucose as an electron donor has been used by Li et al. over ZnS-coated $ZnIn_2S_4$ [62]. Glucose from cellulose or starch only from the viewpoint of renewable sources is better compared to the Na_2S/Na_2SO_3. Various types of sacrificial reagents possess different adsorption abilities and a different number of available protons. In this context, MXenes acts as co-catalyst and show relative efficiency while reacting with sacrificial reagents. MXenes behave as electron acceptors, owing to the lower Fermi level. Hence, the photogenerated electrons flow from the semiconductor to Ti_3C_2. By accumulating electrons at the proper Fermi level, the hydrogen production reaction takes place. The Schottky barrier prevents returning of electrons to the semiconductor surface, which in turn prevents the recombination of charges.

3. Construction of MXene/metal sulfide

3.1. Preparation of MXenes

One of the groups of two-dimensional materials is MXenes, which are composed of carbide, nitride or carbonitride of intermediate metals [63]. The raw material for making MXenes is MAX phase with the general chemical formula $M_{n+1}AX_n$. The MAX phase consists of a primary transition metal (M), an element of groups 13 and 14 of the periodic table (A), and carbon or nitrogen (X) and n is mainly 1, 2, or 3 [64, 65]. To prepare MXenes, selective etching of "A" atoms from the ternary layered $M_{n+1}AX_n$ using an acidic solution containing fluorine such as hydrogen fluoride and lithium fluoride is used [66, 67]. For example, $Ti_3C_2T_x$ multilayer nanosheets are made from pure $Ti_3C_2T_x$ using the following process: A sample of Ti_3AlC_2 in hydrogen fluoride solution is added to a closed Teflon chamber and stirred strongly for several hours at ambient conditions. The products are removed from the Teflon container, filtered under vacuum and then washed with distilled water and EtOH. Finally, the solid obtained is heated in the oven for several hours to dry, as shown in Fig. 4 [68]. The final product of this process is 2D Ti_3C_2 MXene [69]. When Ti_3AlC_2 is added to HF solution, the following reactions occur:

$$Ti_3AlC_2 + 3HF \rightarrow Ti_3C_2 + AlF_3 + 3/2H_2 \quad (5)$$

$$Ti_3C_2 + H_2O \rightarrow Ti_3C_2(OH)_2 + H_2 \quad (6)$$

$$Ti_3C_2 + HF \rightarrow Ti_3C_2F_2 + H_2 \quad (7)$$

With only the assistance of mild sonication, a new pathway was found to increase delamination and exfoliation of Ti_3AlC_2 without any additional intercalation. Multilayer Ti_3AlC_2 etching is performed with LiF + HCl solution easily, and the Ti_2CT_x suspension is obtained in a short time with gentle sonication [70]. After filtration, two dimensional MXene is ready to be heated. Ahmad et al. have been described various approaches for the synthesis of 2D Mxenes such as acid etching method, etching with molten salts, acid etching and intercalation, and electrochemical etching [71]. In addition, Biswas and Alegaonkar comprehensivly have investigated fluoride-free synthesis methods as an another approch for MXenes construction [72]. Also, Li et al. have etched Ti_3AlC_2 with KOH in the presence of a small amount of water in order to delamination and make an ideal 2D MXene [73]. However, most of MXene preparation methods use strong acids for etching, which is harmful to humans and the environment [74]. Therefore, developing a safe and environmentally friendly synthesis process for MXenes is crucial.

In the design of $Ti_3C_2T_x$ composite photocatalysts, coupled material such as transition metal oxide (TMOs) [75], metal-organic framework (MOFs) [76], graphitic carbon nitride (g-C_3N_4) [77], transitient metal sulfide (TMSs) and binary composites [78], have been used. In the following, different methods are described for production of intermediate metal sulfides. In this position, MXenes exhibit two differnet role as repressing the e^-/h^+ recombination and presenting active sites for the redox reactions. Morover, photocatalysts combined with MXenes are an alternative to free noble metal photocatalysts.

3.2. Preparation of MXenes as supported semiconductors

In the various photocatalytic processes, MXene-based semiconductors have been combined with metal sulfide in order to construct nano-semiconductors. Two-dimensional MXenes with high mechanical stability play the role of strong support and co-catalyst for the homogeneous formation of derived substances, good dispersal and limited accumulation of metal sulfide, leading to a shorter distance of charge transfer, which is useful for the separation of photoexcited electron/hole pairs for improved photocatalytic performance. The −OH

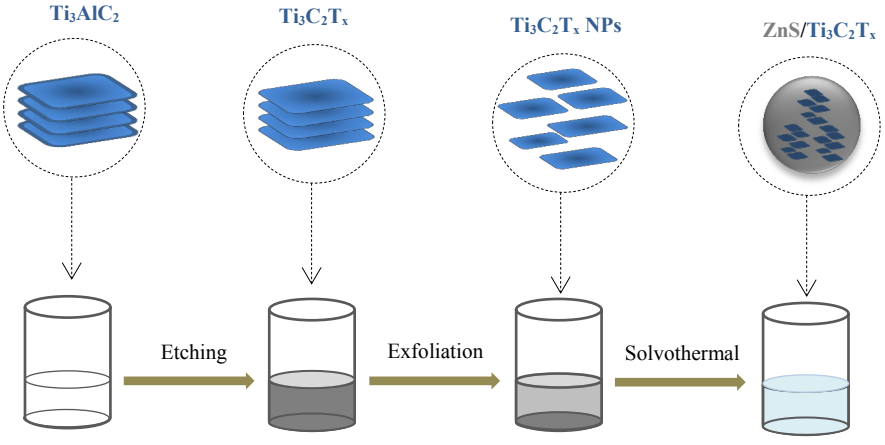

Fig. 4. Illustration of $Ti_3C_2T_x$ preparation.

and –O groups- modified MXenes, especially affect the reaction routs. In general, terminal functional groups, which depend on the synthesis method, alter and control the chemical properties of $Ti_3C_2T_x$ [79]. Importantly, the performance of the work and the transportation characteristics of MXenes can be manipulated by their surface groups (–O, –F, –OH,), which allows adjustable electronic properties by tuning their surface chemistry, which can control MXenes construction of their photocatalytic performance [80]. Desired MXene/metal sulfide nanocomposites can be obtained via hydrothermal/solvothermal process, sole-gel method, calcination technique, and mixing procedure.

3.2.1. Hydrothermal/solvothermal process

The basis of hydrothermal synthesis is the dissolution of materials in water, which under the desired temperature and pressure leads to the production of the product [81]. After dissolving in water, the raw materials are placed in a sealed device called an autoclave, which is often made of stainless steel. The solution is heated to a temperature above the boiling point of water, so the pressure inside the autoclave rises. Over time, during the stirring of the mixture, the growth of the product crystals is complete. The effect of temperature and pressure leads to the production of crystalline materials in a single-step process that does not require any treatment [82]. Adjusting the pH can reduce the generation of undesirable products [83]. In such conditions which are possible to easily control the reaction parameters such as temperature and reaction time, heterocomposites can be produced with high crystal allocation in nano-size. Therefore, this method can easily synthesize MXenes supported semiconductors based photocatalysts.

In the typical preparation process, Ti_3C_2OH is added to distilled water, and then ultrasonic distribution for a few minutes utilizing an ultrasonic cell crusher. $CdCl_2$ and $In(NO_3)_3{\cdot}4H_2O$ are added to the Ti_3C_2OH solution. After industriously stirring for a while, the indium, and cadmium ions are absorbed to the surface of $Ti_3C_2T_x$ to create a homogeneous solution (1^{st} mixture). The hexadecyl trimethyl ammonium bromide and thioacetamide are then dissolved in distilled water and stirred for a few minutes to give a second solution. Immediately, the 2nd solution is gently mixed with the first solution and stirred vigorously in an autoclave for a long time under a high temperature hydrothermal process as shown in Fig. 5 [21]. The resultant $Ti_3C_2T_x$/CdS/In_2S_3 mixture is dried above room temperature.

The hydrothermal synthesis method is superior to other methods used to prepare crystalline phases. Some crystals are not stable at the melting point or have high vapor pressure at their melting point. Therefore, these crystalline species can be prepared by hydrothermal method, while the desired quality product with maintaining its composition is produced [84]. Furthermore, in terms of energy consumption, the price of precursors and control devices, compared to other procedures this method is low cost. In addition, this process offers superiorities such as good dispersion of materials in solution and environmental friendliness.

Despite the above advantages, the hydrothermal method also has disadvantages, including the need for expensive autoclaves. On the other hand, it is not possible to see growing crystals because the autoclave wall is not transparent [85]. These devices withstand up to 300 °C and 1000 kpa pressure. Maintaining safety issues during the reaction should also be considered [86]. Furthermore, the autoclave and seals must be resistant to corrosion by the solution because in most cases corrosive solutions are used in the hydrothermal method.

The solvothermal technique is very similar to the hydrothermal procedure because the technique used is the same in both. The difference between these methods is in the type of solvent used as the reaction medium. In the solvothermal method, organic solvent is used, while in the hydrothermal process water is utilized. On the other hand, organic solvents can stop oxidation, which is especially necessary for the preparation of non-oxides [87]. This method is used to synthesize composite nanocrystals with desirable properties. In addition, the solvothermal procedure is one of the most common and powerful fabrication methods to prepare MXenes-based photocatalysts with different morphology. In this method, reactions are performed above environmental conditions in a sealed autoclave in organic solution.

For example Tie et al. have synthesized ZnS nanoparticles with Ti_3C_2 MXene nanosheets through solvothermal method. At first, they have dissolved thioacetamide (TAA) in glycerol-ethanol solution and stirred at ambient condition for a few minutes [88]. In the following, $ZnCl_2$ and Ti_3C_2 have been added in the organic solution and then the suspension transferred into a seal batch reactor and has heated for several hours at high temperature. The resulting solution has been removed from the autoclave and after cooling, washed with distilled water and alcohol several times and dried in a heater. Thus ZnS/Ti_3C_2 MXene nanosheets have been produced through a method called in-situ decoration for enhanced photocatalytic hydrogen evolution. Furthermore, alcoholic solutions can be synthesized from syngas to prevent greenhouse gas emissions [89].

3.2.2. Sol-gel method

The chemical deposition method, or sol-gel process, was invented in the 19th century and is known in materials science and engineering as a wet chemical technique for the construction of new composites [90]. In this method, a chemical solution is used as a gel or network precursor to create an integrated network structure [91]. Conventional precursors such as metal chlorides and alkoxides are used to synthesize metal

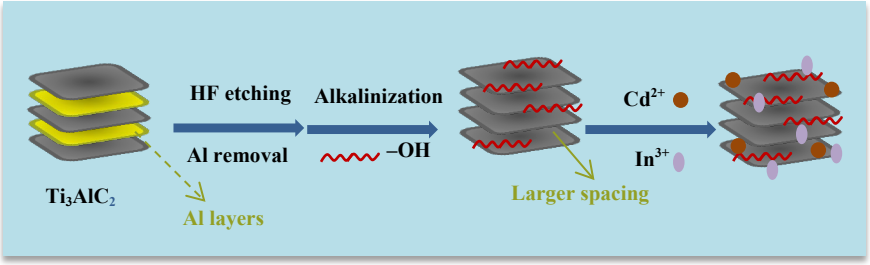

Fig. 5. A brief description of the preparation process for the Ti_3C_2–OH–In_2S_3–CdS.

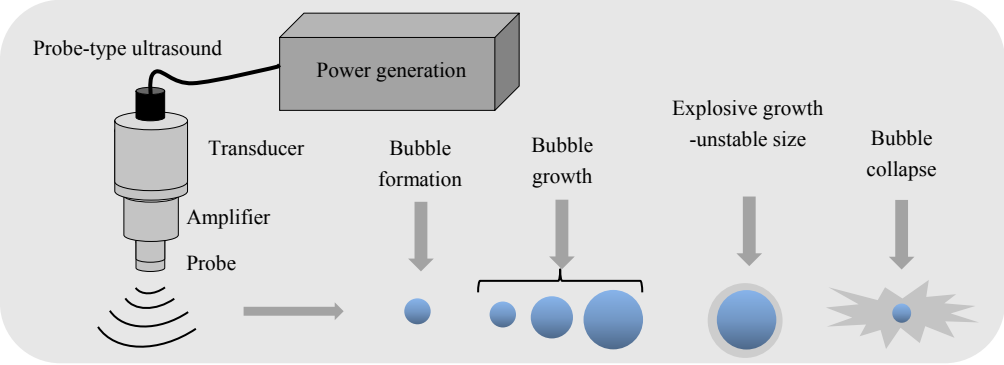

Fig. 6. Schematic of the ultrasonic method and the stages of bubbles formation to its explosion.

sulfides and oxides at the nanoscale. When the precursor solution is passed through the gel, a solid product is formed. The sol-gel method can control the textural and surface properties of composites.

The major advantages of this method are the control of product size, porosity and morphology, low operating temperature, simplicity, cost-effectiveness and efficiency to produce a high quality product. The disadvantages of this method are 1) the use of organic solutions that can be toxic; 2) long processing time; 3) the contraction that occurs during processing; 4) residual hydroxyl and/or carbon groups; and 5) fine pores [91].

For example in a typical sol-gel method, Cu_2SrSnS_4 has been prepared by thiourea, tin chloride, and copper acetate monohydrate solutions. This mixture has been stirred at a desirable temperature in less than an hour to get a dark yellow solution called CTS mixture [92]. Besides, strontium acetate has been added to 2-methoxy ethanol and lactic acid as a fluxing agent in order to reduce agitating time. The Sr solution is then stirred at a temperature below 100 °C to get a colorless translucent solution. The two prepared solutions were then mixed together and stirred at above room temperature for a while to get a translucent yellow precursor solution. Small amounts of triethanolamine and diethanolamine were mixed with the precursor solution as a filmogen and stabilizer. Tetzlaff et al. have also prepared $Fe_xNi_{9-x}S_8$ nanoparticles via the sol-gel method by metal salts, $Ni(NO_3)_2$ and $Fe(NO_3)_3$ in distilled water and citric acid to form a gel [93].

3.2.3. Calcination technique

One of the most ordinary thermal methods for synthesizing ceramic materials is calcination. In this method, the materials are heated under controlled conditions. The calcination technique is also utilized to prepare MXene/nanocomposite in which MXene acts as a cocatalyst. Photocatalytic performance is strongly dependent on the calcination temperature [91].

Since the product of most calcination processes is prepared with pre-designed materials, the particle size, aggregation, and phase composition in the product would be approved. It should also be noted that the calcination process can be combined with other methods such as the microwave method that requires heating [86]. However, because of MXenes oxidation at high temperatures and losing their conductivity, the calcination temperature is the most important process parameter [34]. Therefore, milder conditions should be applied in calcination of substances containing MXenes. Hence, appropriate solutions are essential for the design of ultra-strong heterostructural matter that prevents the oxidation of MXenes.

3.2.4. Ultrasonic method

The basis of the ultrasonic technique is acoustic cavitation, which is used in the preparation of new materials with outstanding properties. In a liquid, the formation of a shock wave generated with a physical force, leads to the constitution of bubbles and the growth and bursting of bubbles, as shown in Fig. 6. The sonochemical synthesis of compounds doesn't require a strong condition (pressure and temperature) or a long time of processing [94].

4. Hydrogen generation via MXenes/metal sulfide

Hydrogen production from the reaction of splitting water under sunlight on the surface of semiconductors is a good way to generate energy because water and sunlight are both renewable. Low-cost photocatalysts, including MXenes, have suitable efficiencies in the hydrogen evolution process, which has a lower Fermi level than other semiconductors. As mentioned earlier, metal sulfides have excellent conduction band and valence band energy levels with high resistance for photocatalysts construction, which are used to produce hydrogen under the visible light illumination. Furthermore, in hybrid systems, MXenes, as a favorable support layer, can be combined with metal sulfides to construct a semiconductor with fine dispersion for increasing photocatalytic activity. In this section, various MXenes-based metal sulfides and their photocatalytic performance in hydrogen generation are summarized. Table 1 presents the diverse photocatalytic activity of MXene/metal sulfide toward H_2 generation. TiO_2 was one of the first semiconductors used in the photocatalytic splitting of water, used in multiple systems. As shown in Table 1, TiO_2 has a significant effect on increasing production efficiency.

Metal sulfides with general MxSy formulas (x and y are integers) are derived from the transplant of a metal or semi-metal cation with sulfur ion, which includes a variety of compounds MS, MS_2, M_2S, M_3S_4. While bimetallic sulfides with $A_{1-x}B_xS_y$ stoichiometry are divided into two general categories that have a different structure. The first group with the AB_2S_4 formula has a cubic spinel structure, and zinc, copper, manganese and so on as divalent metal ions; occupy the metal A site, while the B site is filled with triple metal ions such as indium, cobalt, etc. Several studies claimed that dual metal sulfides ($CdIn_2S_4$, $ZnIn_2S_4$, etc.) with AB_2S_4 can be a new class of active photocatalysts under visible light irradiation. These compounds with M_xS_y and AB_2X_4 structure have been listed in Table 1, with different synthesis method, for photogeneration of H_2.

Table 1. Summary of MXene/metal sulfide for hydrogen evolution.

Photocatalyst system	Synthesis strategy	Light source	Sacrificial reagent	Conditions	Activity ($\mu mol.g^{-1}.h^{-1}$)	Note	Ref.
CdS & ZnS							
ZnS nanoparticles/$Ti_3C_2T_x$ nanosheets	Etching/ultrasonic exfoliation/solvothermal	300 W Xe lamp, $\lambda > 400$ nm	Lactic acid/ H_2O = 1/4 v/v	Room temperature	502.6	It is evident that $ZT_{0.75}$ displays an increased average lifetime	[88]
CdS/ $Ti_3C_2T_x$ nanoparticles	Hydrothermal	300 W xenon arc lamp, $\lambda \geq 420$ nm	18 vol% lactic acid (LA)	Ambient condition	14342	Quantum efficiency of 40% @ 420 nm	[95]
1D/2D CdS-$Ti_3C_2T_x$	One-step electrostatic self-assembly	300 W xenon lamp ($\lambda > 420$ nm)	Ethanol/H_2SO_4		15400	$^{\bullet}CH_3(OH)CH$ is the pivotal radical species during photocatalysis.	[96]
1D CdS/2D Ti_3C_2	In situ assembling (self-assembly) solvothermally, ultrasonication	300 W xenon lamp with cut-off filter ($\lambda > 420$ nm)	10 wt% lactic acid	6 °C	2407	AQY: 35.6% @ 420 nm	[97]
2D/2D CdS NS@Ti_3C_2 MXene					1730	CdS NSs (0.37 $mmol.h^{-1}.g^{-1}$)	[98]
MXene@Au@CdS					17070.4		[99]
Plasma $Ti_3C_2T_x$/CdS	Etching Al/solvothermal	300 W Xe lamp, $\lambda > 420$ nm	Lactic acid 10 vol%	Ambient condition	825	Quantum efficiency of 10.2% @ 450 nm	[100]
CoO@ Ti_3C_2@CdS hierarchical tandem p-n heterojunction	HF etching/ hydrothermal	300 W Xe lamp, $\lambda = 420$ nm	Without any sacrificial agents	6 °C	134.46		[101]
Mo_2C-MXene/CdS					17964		[102]
$BiVO_4$-CdS-$Ti_3C_2T_x$	Etching by HCl + LiF/Ultrasonication treatment/ solvothermal treatment	300 W xenon lamp, $\lambda > 420$ nm	$AgNO_3$		866.5		[103]
$Ti_3C_2T_x$/CdS	Electrostatic self-assembly process and solvothermal method	300 W Xe lamp, $\lambda > 420$ nm	LA		3226		[104]
ZnS/Ti_3C_2 MXene	Ultrasonic oscillation	300 W Xe lamp, $\lambda < 420$ nm			212 $\mu mol.h^{-1}$		[105]
MoS_2 & WS_2							
$Ti_3C_2/TiO_2/MoS_2$ (loading amount 10, 15, and 25 wt%)	Two-step hydrothermal	300 W Xe arc lamp, AM 1.5 filter	Triethanolamine	25 °C	6425.3		[106]
1T-MoS_2 nanopatch/Ti_3C_2/TiO_2 nanosheet	Hydrothermal	300 W Xe arc lamp, AM-1.5 filter	Acetone/ triethanolamine	25 °C	9738	Quantum efficiency < 6.86%	[107]
Mo_xS@TiO_2@Ti_3C_2	Hydrothermal	300 W Xe arc lamp, AM-1.5 filter	Acetone/ triethanolamine		10505.8	Quantum efficiency < 7.535%	[108]
MoS_2/Ti_3C_2	Hydrothermal	300 W Xe lamp, $\lambda > 420$ nm	CH_3OH		6144.7		[109]
R-scheme Ti_3C_2 MXene/MoS_2 (NS)	Hydrothermal	300 W Xe lamp, $\lambda < 420$ nm	0.35 M Na_2S, 0.25 M Na_2SO_3	Room temperature, atmospheric pressure	380.2		[110]
TiO_2@ $Ti_3C_2T_x$@1T–WS_2	Hydrothermal	300 W Xe arc lamp, AM-1.5 filter	Acetone/ triethanolamine	Room temperature	3409.8	Quantum efficiency < 2.464%	[111]

Table 1. Continued.

Photocatalyst system	Synthesis strategy	Light source	Sacrificial reagent	Conditions	Activity ($\mu mol.g^{-1}.h^{-1}$)	Note	Ref.
Pseudobinary metal sulfide semiconductors							
$ZnIn_2S_4$ (ZIS)/TiO_2/Ti_3C_2	2 step hydrothermal	300 W xenon lamp	0.25 M Na_2SO_3 and 0.35 M $Na_2S.9\ H_2O$	Atmospheric pressure and room temp.	1185.8	The position of the ZIS n-type and TiO_2 conduction bands is slightly more negative than that of Ti_3C_2.	[112]
Ultrathin $ZnIn_2S_4$ nanosheets (UZNs)/$Ti_3C_2T_x$ nanosheets (MNs)	In situ growth	$\lambda \geq 420$ nm			3475		[113]
$Zn_2In_2S_5$/Ti_3C_2 (O, OH)$_x$ (ZIS-MX)	In situ growth/ hydrothermal	300 W Xe arc lamp, $\lambda \geq 420$ nm	0.35 M NaS, 0.25 M Na_2SO_3	Room temperature	12983.8	AQE of 8.96% @ 420 nm	[114]
$Zn_2In_2S_5$/MXene (2.5 wt%)	Etching by HF/ in-situ growth	300 W xenon lamp, $\lambda \geq 400$ nm	Triethanolamine (10 vol%)	8 °C	3042		[115]
2D/2D $Ti_3C_2T_x$/N-$ZnIn_2S_4$ (N-ZIS)	Electrostatic self-assembly/ hydrothermal method	300 W xenon lamp, $\lambda \geq 400$ nm	Triethanolamine	25 °C	148.4		[116]
$Zn_{0.5}Cd_{0.5}S$ (2 wt%)/TiO_2/Ti_2C	Co-precipitation-hydrothermal for $Zn_{0.5}Cd_{0.5}S$, solid reaction sintering for Ti_2AlC	300 W Xe lamp, $\lambda \geq 400$ nm	0.3 M Na_2SO_3– 0.3 M Na_2S	Room temperature	32570	Gibbs free energy of $Zn_{0.5}Cd_{0.5}S$ is higher than oxygen-terminated TiO_2 and Ti_2C.	[117]
MXene/$Zn_xCd_{1-x}S$	Etching by HF/ solvothermal	300 W Xe lamp, $\lambda > 400$ nm	Alkaline polyethylene terephthalate (PET) solution		14170		[118]
$Cd_{0.5}Zn_{0.5}S$/Ti_3C_2 Schottky catalyst	Etching by HF/ hydrothermal	300 W Xe lamp, $\lambda \geq 400$ nm	0.25 M Na_2SO_3 and 0.35 M Na_2S	Room temp. and vacuum condition	9071	quantum efficiency 43.28% @ 420 nm	[119]
$Cd_xZn_{1-x}S$/Ti_3C_2	Etching by HF/hydrothermal	300 W Xe arc lamp, $\lambda > 420$ nm	Na_2S and Na_2SO_3 (1:1 v/v)	5 °C	15035.8	The electron trap is created by a Schottky junction and prevents electrons from returning.	[120]
$CdLa_2S_4$/Ti_3C_2	Etching Ti_3AlC_2 and ultrasonic exfoliation/in situ growth solvothermal	300 W xenon lamp, $\lambda > 420$ nm	0.35 M Na_2S and 0.25 M Na_2SO_3	Room temperature	11182.4	AQE of 15.6% @ 420 nm	[121]
Ti_3C_2 MXene/TiO_2/$CuInS_2$ Schottky-step-scheme (S-scheme) heterojunction	Two-step hydrothermal				356.3	The heterojunction structure can maintain its efficiency in multiple cycles.	[122]
Miscellaneous metal sulfides							
TiO_2-Ti_3C_2-MOF derived CoS_x	Solvothermal	$\lambda \geq 420$ nm	Methanol		950	The color of the sample depends on the amount of Ti_3C_2, the higher its content, the material would be darker and the less light it absorbs.	[123]
CuS/MXene	Facile wet-chemical procedure	300 W Xe lamp, $\lambda \geq 420$ nm	0.25 M of Na_2SO_3 and 0.35 M of Na_2S		4.2	A sample with a Ti:S = 1:2 ratio has the highest photocatalytic activity in hydrogen production.	[124]

4.1. CdS and ZnS

The structural and bonding shape of CdS and ZnS crystals varies depending on their synthesis method and mineral source [125, 126]. Among numerous semiconductor photocatalyst, CdS is nominated as the most prominent and studied candidate for photosplitting of water [127]. Although CdS has a high charge recombination potential, it is an excellent choice for photocatalyst usage due to its small bandgap and corresponds well with the solar irradiation spectrum [128]. But the disadvantage of ZnS and CdS is photocorrosion, which increases in radiation cycles [129]. Sulfur ions oxidize through holes created by sunlight rays to produce cadmium and zinc ions. Moreover, for enhancing light absorption capacity and stability it is recommended to couple CdS with MXenes for enhancing light harvesting capacity. ZnS as a suitable semiconductor with 3.7 eV bandgap shows suitable physical properties and quantum efficiency. In addition, the unique characterize of ZnS nanoparticles have led to its widespread use in photocatalytic processes under visible light radiation [130].

CdS and ZnS as transition metal sulfides coupling with $Ti_3C_2T_x$ have been demonstrated as potential co-catalysts for photocatalytic hydrogen evolution process. In this regard, photocatalytic activity of multidimensional heterojunction of 1D CdS nanorods/2D Ti_3C_2 nanosheets has been investigated by Xiao et al. [97]. They have shown that heterostructure of 1D/2D co-catalyst without any noble metal could be suitable for H_2 evolution under visible light spectrum. In another research, it has been prove that without visible light irradiation or CdS-MX photocatalyst no activity toward H_2 production [96]. The activity of photocatalytic redox reaction improves in the acidic environment and hydrogen produces due to conversion of ethanol. The rate of hydrogen production in the presence of EtOH and sulfuric acid as electron donor is much higher than lactic acid. Additionally, when utilizing single $Ti_3C_2T_x$ alone as a catalyst, no reaction accrues, indicating that CdS nanowires are the only photoactive material in the CdS-MXene compound. Also, Chen et al. have shown that the activity of CdS NS@Ti_3C_2 composite is 4.7 times higher than that of pure CdS NSs under the same conditions [98]. Of course, ZnS/MXene has the advantage of maintaining photocatalytic activity after five test cycles [105] which makes it competitive with CdS.

Nanoparticles of Au as precious noble metal are useful co-catalysts to increase the photocatalytic performance of CdS due to its local surface plasmon resonance. The photoexited electrons on the surface of the gold can be entered by stimulating surface plasmon to the conductive band of cadmium sulfide, which leads to increased photocatalyst efficiency. Furthermore, the noble metal position also significantly affects H_2 evolution during photocatalysis [131]. Furthermore, Ti_3C_2 boosts the number of active sites and reaction centers for CdS and Au nanoparticles [99]. However, noble metal co-catalyst utillized in photoevolving H_2 is high-cost and difficult to obtain. As shown in Table 1, MXene@Au@CdS has the highest hydrogen production rate compared to other photocatalysts. Pore size, pore volume and the BET surface area of Au/CdS/MXene, indicating that loading Au/CdS nanosized with MXenes provides a porous structure and numerous active sites for H_2 generation. The illustration of Au/CdS/MXene fabrication and H_2 generation is shown in Fig. 7.

4.2. MoS_2 & WS_2

Other semiconductors such as MoS_2 [132] and WS_2 [133] from group 6 of the periodic table as a class of transition metal sulfides, which is used in photocatalytic hydrogen evolution. The pairing of these materials with MXenes increases the photocatalytic activity several times compared to single metal sulfide. MoS_2 has little oxidation potential so its photocatalytic activity is insufficient. But the MoS_2 nanostructure has the ability to change the valence band to increase the efficiency of the photocatalytic process, which has been attributed to the quantum confinement of nanomaterials [134]. Hydrothermally prepared MoS_2/Ti_3C_2 heterostructure composite exhibited the highest hydrogen generation rate, which are 2.3 times higher than those of the pure MoS_2 and still maintains high activity after four cycles [109]. The heterostructure, in addition to creating more active sites, effectively reduces recombination of electron/hole pairs.

Titania is one of the most suitable semiconductor in photocatalytic production of hydrogen, along with MXene, has an effective heterogenic structure for the separation of charging carriers. Titania is the only semiconductor that is traditionally prepared via in-situ oxidation, combined with Ti_3C_2 as a precursor. As ternary systems have been attracted much attention as the hopeful system for enhancing

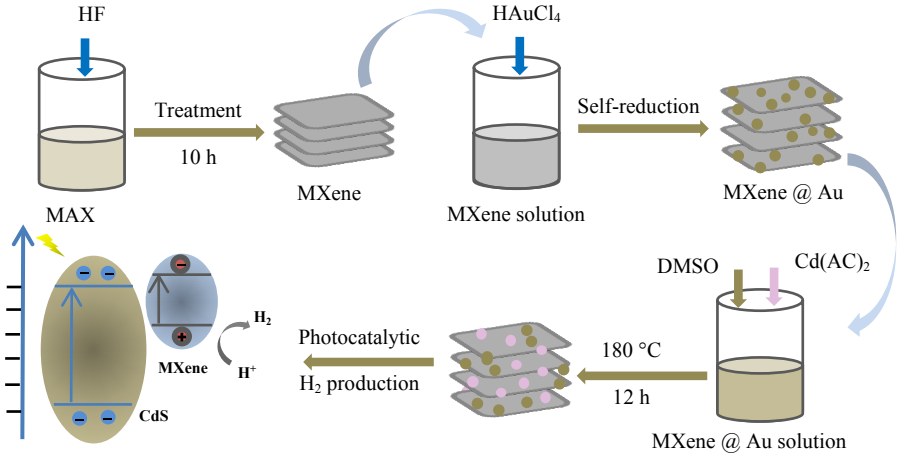

Fig. 7. Schematic of the MXene@Au@CdS preparation flow chart and energy band structure diagram.

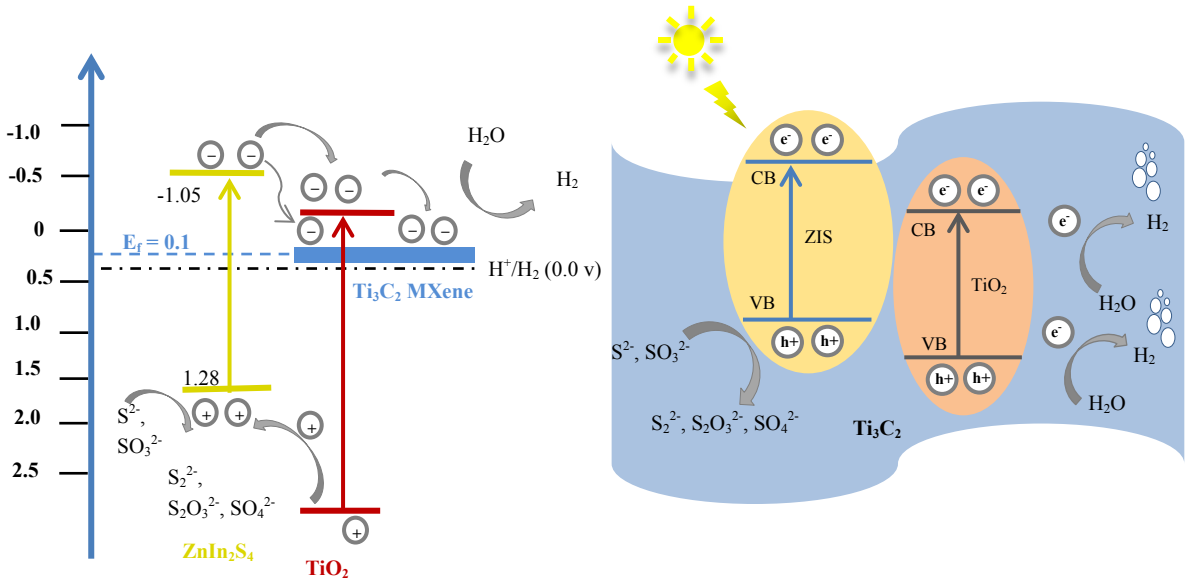

Fig. 8. a) Schematic of electrons and holes transfer flow over $TiO_2/Ti_3C_2/ZnIn_2S_4$ and b) schematic of photocatalytic hydrogen evolution mechanism on $TiO_2/Ti_3C_2/ZnIn_2S_4$.

photocatalytic activity, so Li et al. have reported the H_2 evolution by $Ti_3C_2/TiO_2/1T\text{-}MoS_2$ [107]. By optimal loading amount of MoS_2, the rate of hydrogen production by $Ti_3C_2/TiO_2/1T\text{-}MoS_2$ can be 1.5, 11, and 132 times higher than that of TiO_2/2H-MoS_2 (hexagonal), TiO_2/Ti_3C_2 and pure titania. Structural form 2H type has hexagonal symmetry with trigonal prismatic arrangement, which repeat per two layers. Another example of ternary systems in this group of metals, WS_2 and Ti_3C_2 decorated with TiO_2 as dual metallic co-catalysts could facilitate transfer of photoexited e^- and timely consume h^+ produced by sacrificial reagent [108]. The prominent activity of the 1T-WS_2 Ti_3C_2/TiO_2 can be attributed to the easy transfer of electrons produced by light and the convenient consumption of holes produced by electron donors.

4.3. Pseudobinary sulfide solution

Several studies claimed that dual metal sulfides ($CdIn_2S_4$, $ZnIn_2S_4$, etc.) with AB_2S_4 can be a new class of active photocatalysts under visible light irradiation. During recent years, Cd_xZn_yS and Zn_xIn_yS as bimetallic sulfides have been considered a lot of attention to the production of photocatalytic hydrogen. However, rapid recombination of the electron/hole pairs strongly limits the performance of these single-semiconductors. To fix this disadvantage, the combination of semiconductor photocatalysts with MXenes to build heterojunctions effectively increases electron/hole pair's separation. Generally, bimetallic sulfides have three structural shape species: trigonal (1T), hexagonal (2H) and rhombohedral (3R). The trigonal and hexagonal forms as photocatalyst materials have been studied for H_2 solar driven [135, 136].

The bandgap of bimetal sulfides can be changed by structural modification. Hence the geometric shape and number of layers have a great effect on the bandgap [137, 138]. Also, bimetal sulfides are very similar to graphite and have a two-dimensional structure that affects their chemical, thermal and electrical properties [139]. Because the number of layers can be changed easily, the bandgap in this material is adjustable. Therefore, bimetal sulfides are a good alternative to precious noble metals.

One of the bimetal sulfides of interest is $Zn_xCd_{1-x}S$, which has been used in the hydrogen production process under visible light irradiation. This type of sulfide has excellent photocatalytic properties, is photo-corrosion resistant and has the ability to adjust the bandgap. $Zn_xCd_{1-x}S$ photocatalysts are a combination of wurtzite and zinc, which have a unique crystal structure and have recently been used as bimetal calcogenides in the water-splitting reaction. Recently, studies have been conducted to increase the efficiency of hydrogen production by combining this photocatalyst with a base co-catalyst [140]. The solid solution of $Zn_xCd_{1-x}S$ is formed as a result of the structural similarity of cadmium sulfide and zinc sulfide, the high solubility of which has been attributed to this reason [141]. By controlling the stoichiometric coefficient of zinc and cadmium, the band gap of $Zn_xCd_{1-x}S$ can be changed [142].

$Cd_{0.7}Zn_{0.3}S$ is one of the best photocatalysts reported in the hydrogen production process without any co-catalysts under the visible light illumination, which has a high ability to separate charge carriers compared to other photocatalysts [143]. However, by growing $Zn_{0.5}Cd_{0.5}S$ nanoparticles on TiO_2/Ti_2C, hydrogen production is increased more than 10 times [117].

Another type of metal sulfide is $ZnIn_2S_4$, which has reduced the recombination rate of charge carriers with various strategies such as morphological control, surface modification, doping with metal ions and formation of heterogeneous structure [144]. Huang et al. reported that combining this photocatalyst with TiO_2/MXene could prevent electron reversal and speed up the transfer of electrons from $ZnIn_2S_4$ to MXene, as shown in Fig. 8 [112].

4.4. Mixed metal sulfides

To date, there are few studies on the bi-loading strategy of metal sulfides with MXenes. However, loading two metal sulfides imposes a strong synergistic enhancement on the separation of charge carriers and

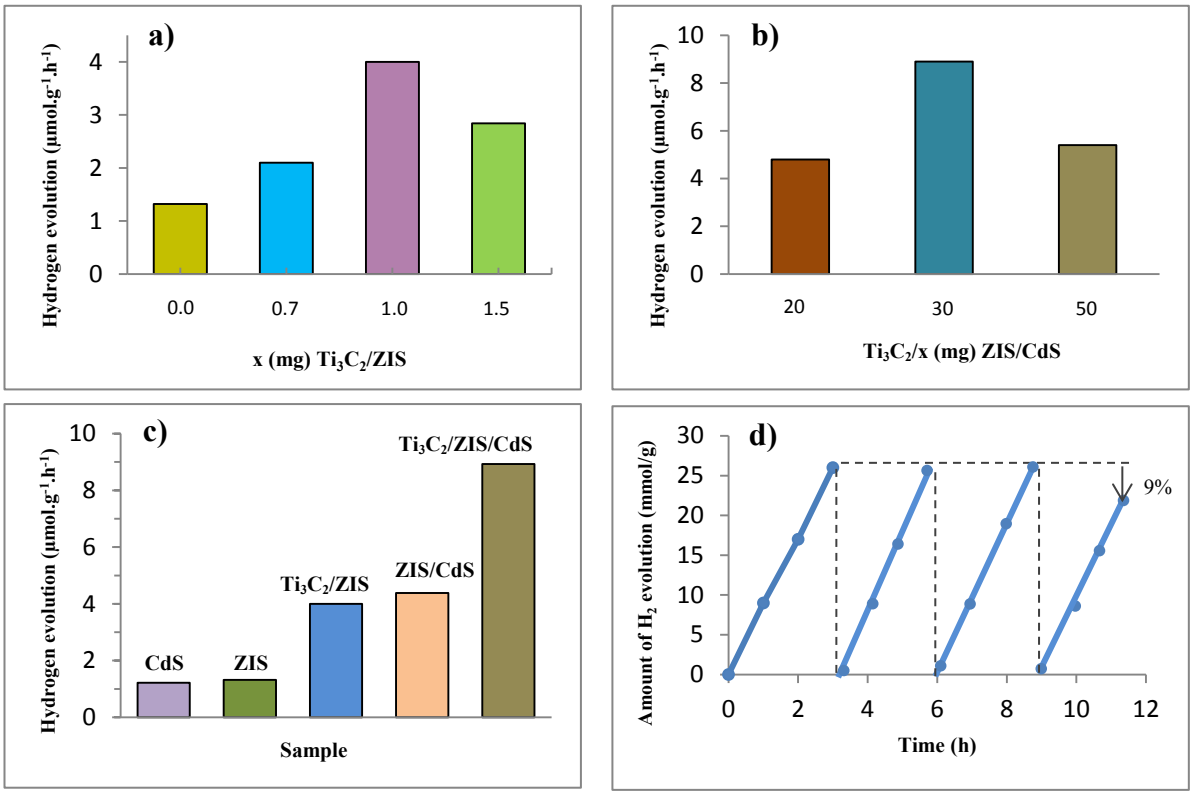

Fig. 9. a) Diagram of the effect of Ti_3C_2 loaded on H_2 production with $ZnIn_2S_4$ photocatalyst, b) H_2 production rate over different amount of $ZnIn_2S_4$ on CdS/ Ti_3C_2, c) H_2 production rate in the vicinity of CdS, $ZnIn_2S_4$, $ZnIn_2S_4/Ti_3C_2$, $CdS/ZnIn_2S_4$ and $CdS/ZnIn_2S_4/Ti_3C_2$, and d) $ZnIn_2S_4/CdS/Ti_3C_2$ capability in alternating cycles.

transfer in photocatalyst [95]. The results demonstrate the great potential of loading Ti_3C_2 with other co-catalysts to achieve the synergetic effect of photocatalytic performance. Summary of mixed metal sulfides/MXenes are presented in Table 2.

For example, the $Ti_3C_2/ZnIn_2S_4/CdS$ S-scheme photocatalyst exposes hydrogen-evolution rate about 7.32 and 6.77 times higher than those of CdS and $ZnIn_2S_4$, respectively (Fig. 9) [145]. The prepared $Ti_3C_2/ZnIn_2S_4/CdS$ composite photocatalyst by a two-step solvothermal method exhibits good stability during continuous photocatalytic H_2 generation. The S-scheme photocatalytic system can effectively overcome the defects of unitary photocatalyst and a typical type II heterojunction, improve the light absorption range and redox capacity, and promote its charge separation ability.

In another mixed system, Chen et al. have synthesized of CdS/MoS_2/MXenes by an easy hydrothermal process for photocatalytic H_2 generation [147]. Fig. 10 shows the photocatalytic performance of CdS-MoS_2 with the MXene cocatalyst, which is much faster than hydrogen metal sulfide alone. Even MXene-free hybrid photocatalysts are much less efficient, suggesting that MXene plays an effective role in transporting charge carriers and reducing their recombination rate.

Table 2. Mixed metal sulphides co-catalyst with MXene for the photocatalytic H_2 evolution.

Photocatalyst system	Synthesis strategy	Light source	Sacrificial reagent	Conditions	Activity ($\mu mol.g^{-1}.h^{-1}$)	Note	Ref.
Ti_3C_2/NiS (2.5% mol)/CdS (1 mol%)		300 W Xe lamp, $\lambda \geq 420$ nm	Lactic acid 18%		18560		[95]
2D/2D $ZnIn_2S_4$/CdS S-scheme	Two step solvothermal	300 W Xe lamp, $\lambda > 420$ nm	TEOA		8930	AQE of 3.42% at 420 nm	[145]
$Ti_3C_2(TiO_2)$/CdS/MoS_2	Facile hydrothermal				8470		[146]
CdS-MoS_2/Ti_3C_2	Hydrothermal/ ultrasonication	300 W xenon lamp, $\lambda \geq 420$ nm	0.35 M of Na_2SO_3 and 0.25 M of Na_2S		9679	Quantum efficiency of 26.7% @ 420 nm	[147]

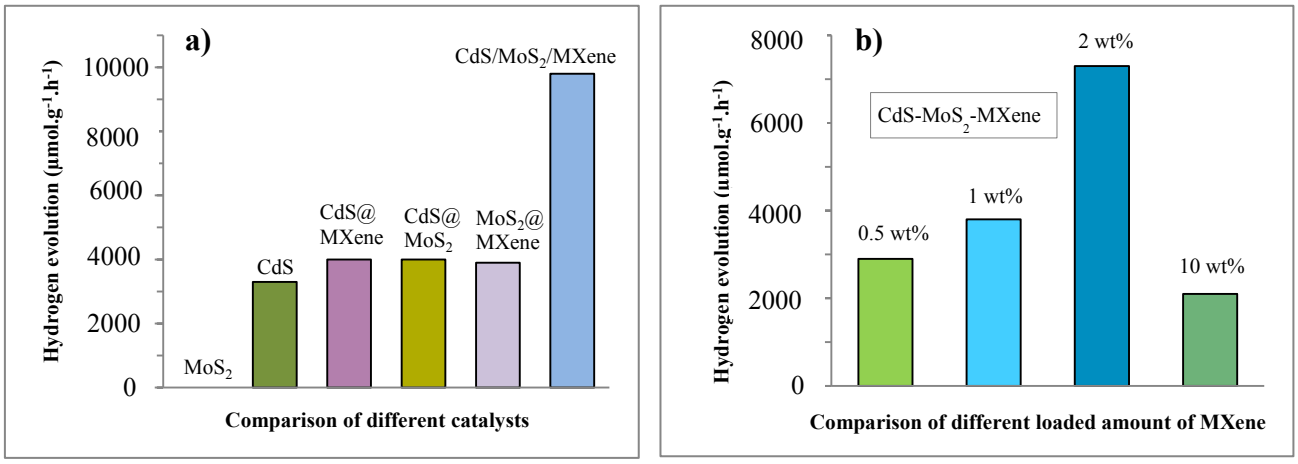

Fig. 10. a) Comparison of the H_2 production rate over metal sulfide, bimetal sulfide, MXene-metal sulfide and MXene-bimetal sulphide photocatalysts and b) The effect of the amount of MXene loaded as a cocatalyst on the rate of hydrogen production with the MoS_2-CdS photocatalyst.

5. Conclusions and outlook

In summary, this review highlighted advances over the MXene/metal sulfide composite in the field of photocatalytic H_2 production. The basic principle of photocatalysis and the role of MXenes-based metal sulfide in hydrogen evolution with the design and development of research were described. Moreover, MXenes preparation procedure and metal sulfide synthesis through different method such as hydrothermal, solvothermal and precipitation technique were presented. Furthermore, in the surface of the MXenes-based metal sulfide, which be preserved by terminal groups (i.e., –O, –OH, and –F), the solvent can be easily removed from the surface and the electron/hole pairs rapidly separated in the metal sulfide. However, the highest photocatalytic activity is obtained with $Ti_3C_2T_x$ having the –O factor group at the end.

In general, MXenes act as the electron sink, electronic promoter and electron/hole transporter, to receive the photoexcited e^- from semiconductor quickly. Ti_3C_2 is one of the most popular and considered MXenes, due to the appropriate Fermi level, act as a co-catalyst in hydrogen evolution from water splitting reaction. The metal sulfides in the presence of MXene especially $Ti_3C_2T_x$ have a better efficiency to perform the evolution of hydrogen. Notably, surface terminal groups of $Ti_3C_2T_x$ and coupling with metal sulfides such as CdS, ZnS, WS_2, MoS_2, etc. alter photocatalytic properties of Ti_3C_2. Nevertheless, there is still a long way to go to produce on an industrial scale and practical application. The future development of MXenes requires finding a new way to produce in milder conditions that vital lower temperatures and etchant with lower toxicity mixtures, such as LiF–HCl for scalability and stability. However, preparation methods should be developed without the need for HF, which may lead to progress in the properties of MXenes.

Various parameters such as selecting the appropriate photocatalyst, type of sacrificial reagent, design of photo-reactor and radiation source play an important role in the efficiency of the hydrogen production process. The type of photocatalyst directly affects the amount of hydrogen production activity. In addition, different types of sacrificial reagents as electron donors have different ability of proton absorption. As a result, each photocatalyst has a different performance depending on the type of sacrificial reagent. In addition to the reaction parameters, the photocatalyst structure, defect engineering and morphology are involved in achieving higher photocatalytic H_2 production efficiency.

The presence of a functional group in Ti_3C_2 can cause many changes in its properties. Also, further functionalization and construction of new functional groups at the end of Ti_3C_2 can improve the photocatalytic properties. Moreover, photocatalytic activity can be further enhanced by coupling with novel metal sulfides and boost their potential as co-catalyst for energy storage. Through structural engineering, the lifespan of the photocatalyst and its stability for use in multiple cycles should be increased. In MXene synthesis, morphological control can be an effective factor in increasing the number of active sites. Pieced MXenees with different morphological structures such as nanorods, quantum dots, and spheres have a larger surface area than a multilayer structure. Therefore, more research should be developed on structural and morphological control.

With the development of material description techniques, the analysis of MXenes structures will become better and easier, both quantitatively and qualitatively under the photocatalysis process. Along with the study of MXenes-based metal sulfides that play a key role in photocatalytic activity, the impress of the terminal MXenes functional group must also be carefully considered. In this regard, it is necessary to understand the physicochemical characteristic of sulfide photocatalysts based on MXenes types. It seems that in the field of energy production and solving the challenges of fossil fuels, photocatalysts composed of metal sulfides, along with the co-catalyst MXenes, can have a promising future for the production of green hydrogen, but extensive research must be done for developing and industrialize the process.

CRediT authorship contribution statement

Asieh Akhoondi: Writing – original draft.
Hadi Ghaebi: Writing – review & editing.
Lakshmanan Karuppasamy: Writing – review & editing.
Mohammed M. Rahman: Writing – review & editing, Supervision.
Panneerselvam Sathishkumar: Writing – review & editing.

Data availability

As this is a review article, no new data were generated or analyzed. All information and data sources referenced are publicly available or cited appropriately within the article.

Declaration of competing interest

The authors declare no competing interests.

Funding and acknowledgment

This research received no external funding. The authors have no acknowledgments to declare.

References

[1] T. Hisatomi, J. Kubota, K. Domen, Recent advances in semiconductors for photocatalytic and photoelectrochemical water splitting, Chem. Soc. Rev. 43 (2014) 7520–7535. https://doi.org/10.1039/C3CS60378D.

[2] B. Su, F. Lin, J. Ma, S. Huang, Y. Wang, et al., System integration of multi-grade exploitation of biogas chemical energy driven by solar energy, Energy. 241 (2022) 122857. https://doi.org/10.1016/j.energy.2021.122857.

[3] T. Hisatomi, K. Takanabe, K. Domen, Photocatalytic Water-Splitting Reaction from Catalytic and Kinetic Perspectives, Catal. Lett. 145 (2015) 95–108. https://doi.org/10.1007/s10562-014-1397-z.

[4] V.K.H. Bui, T.N. Nguyen, V.V. Tran, J. Hur, I.T. Kim, et al., Photocatalytic materials for indoor air purification systems: An updated mini-review, Environ. Technol. Innov. 22 (2021) 101471. https://doi.org/10.1016/j.eti.2021.101471.

[5] A.V. Zaitsev, I.A. Astapov, Prospects for creating regenerated photocatalytic materials for solar water treatment units, Mater. Lett. 310 (2022) 131509. https://doi.org/10.1016/j.matlet.2021.131509.

[6] G. Zhang, C.D. Sewell, P. Zhang, H. Mi, Z. Lin, Nanostructured photocatalysts for nitrogen fixation, Nano Energy. 71 (2020) 104645. https://doi.org/10.1016/j.nanoen.2020.104645.

[7] Z. Fu, Q. Yang, Z. Liu, F. Chen, F. Yao, et al., Photocatalytic conversion of carbon dioxide: From products to design the catalysts, J. CO2 Util. 34 (2019) 63–73. https://doi.org/10.1016/j.jcou.2019.05.032.

[8] X. Ma, H. Cheng, Facet-dependent photocatalytic H2O2 production of single phase Ag3PO4 and Z-scheme Ag/ZnFe2O4-Ag-Ag3PO4 composites, Chem. Eng. J. 429 (2022) 132373. https://doi.org/10.1016/j.cej.2021.132373.

[9] R.M.N. Yerga, M.C. Alvarez-Galván, F. Vaquero, J. Arenales, J.L.G. Arenales, Hydrogen Production from Water Splitting Using Photo-Semiconductor Catalysts, Renewable Hydrogen Technologies, Elsevier. (2013) 43–61. https://doi.org/10.1016/B978-0-444-56352-1.00003-9.

[10] S. Asadzadeh-Khaneghah, A. Habibi-Yangjeh, M. Shahedi Asl, Z. Ahmadi, S. Ghosh, Synthesis of novel ternary g-C3N4/SiC/C-Dots photocatalysts and their visible-light-induced activities in removal of various contaminants, J. Photochem. Photobiol. A. 39 (2020) 112431. https://doi.org/10.1016/j.jphotochem.2020.112431.

[11] B. Mazinani, A. Beitollahi, A.K. Masrom, L. Samiee, Z. Ahmadi, Synthesis and photocatalytic performance of hollow sphere particles of SiO2-TiO2 composite of mesocellular foam walls, Ceram. Int. 43 (2017) 11786–11791. https://doi.org/10.1016/j.ceramint.2017.06.017.

[12] V.-H. Nguyen, M. Mousavi, J.B. Ghasemi, Q.V. Le, S.A. Delbari, et al., High-impressive separation of photoinduced charge carriers on step-scheme ZnO/ZnSnO3/Carbon dots heterojunction with efficient activity in photocatalytic NH3 production, J. Taiwan Inst. Chem. Eng. 118 (2021) 140–151. https://doi.org/10.1016/j.jtice.2021.01.012.

[13] V.-H. Nguyen, M. Mousavi, J.B. Ghasemi, Q.V. Le, S.A. Delbari, A. Sabahi Namini, Novel p–n Heterojunction Nanocomposite: TiO2 QDs/ZnBi2O4 Photocatalyst with Considerably Enhanced Photocatalytic Activity under Visible-Light Irradiation, J. Phys. Chem. C. 124 (2020) 27519–27528. https://doi.org/10.1021/acs.jpcc.0c08316.

[14] C. Xia, T.H.C. Nguyen, X.C. Nguyen, S.Y. Kim, D.L.T. Nguyen, et al., Emerging cocatalysts in TiO2-based photocatalysts for light-driven catalytic hydrogen evolution: Progress and perspectives, Fuel. 307 (2022) 121745. https://doi.org/10.1016/j.fuel.2021.121745.

[15] X. Li, W. Zhang, J. Li, G. Jiang, Y. Zhou, et al., Transformation pathway and toxic intermediates inhibition of photocatalytic NO removal on designed Bi metal@defective Bi2O2SiO3, Appl. Catal. B. 241 (2019) 187–195. https://doi.org/10.1016/j.apcatb.2018.09.032.

[16] D.J. Martin, N. Umezawa, X. Chen, J. Ye, J. Tang, Facet engineered Ag3PO4 for efficient water photooxidation, Energy Environ. Sci. 6 (2013) 3380–3386. https://doi.org/10.1039/C3EE42260G.

[17] T. Wei, J. Xu, C. Kan, L. Zhang, X. Zhu, Au tailored on g-C3N4/TiO2 heterostructure for enhanced photocatalytic performance, J. Alloys Compd. 894 (2022) 162338. https://doi.org/10.1016/j.jallcom.2021.162338.

[18] Y.-P. Yuan, L.-S. Yin, S.-W. Cao, G.-S. Xu, C.-H. Li, C. Xue, Improving photocatalytic hydrogen production of metal–organic framework UiO-66 octahedrons by dye-sensitization, Appl. Catal. B. 168–169 (2015) 572–576. https://doi.org/10.1016/j.apcatb.2014.11.007.

[19] M. Khazaei, M. Arai, T. Sasaki, C.-Y. Chung, N.S. Venkataramanan, et al., Novel Electronic and Magnetic Properties of Two-Dimensional Transition Metal Carbides and Nitrides, Adv. Func. Mater. 23 (2013) 2185–2192. https://doi.org/10.1002/adfm.201202502.

[20] P. Kuang, Z. Ni, J. Yu, J. Low, New progress on MXenes-based nanocomposite photocatalysts, Mater. Rep: Energy. 2 (2022) 100081. https://doi.org/10.1016/j.matre.2022.100081.

[21] H. Fang, Y. Pan, M. Yin, L. Xu, Y. Zhu, C. Pan, Facile synthesis of ternary Ti3C2–OH/ln2S3/CdS composite with efficient adsorption and photocatalytic performance towards organic dyes, J. Solid State Chem. 280 (2019) 120981. https://doi.org/10.1016/j.jssc.2019.120981.

[22] J. Ji, L. Zhao, Y. Shen, S. Liu, Y. Zhang, Covalent stabilization and functionalization of MXene via silylation reactions with improved surface properties, FlatChem. 17 (2019) 100128. https://doi.org/10.1016/j.flatc.2019.100128.

[23] M. Naguib, M. Kurtoglu, V. Presser, J. Lu, J. Niu, et al., Two-Dimensional Nanocrystals Produced by Exfoliation of Ti3AlC2, Adv. Mater. 23 (2011) 4248–4253. https://doi.org/10.1002/adma.201102306.

[24] R. Syamsai, J.R. Rodriguez, V.G. Pol, Q.V. Le, K.M. Batoo, et al., Double transition metal MXene (TixTa4−xC3) 2D materials as anodes for Li-ion batteries, Sci. Rep. 11 (2021) 688. https://doi.org/10.1038/s41598-020-79991-8.

[25] X. Li, X. Ma, Y. Hou, Z. Zhang, Y. Lu, et al., Intrinsic voltage plateau of a Nb2CTx MXene cathode in an aqueous electrolyte induced by high-voltage scanning, Joule. 5 (2021) 2993–3005. https://doi.org/10.1016/j.joule.2021.09.006.

[26] X. Zhai, H. Dong, Y. Li, X. Yang, L. Li, et al., Termination effects of single-atom decorated v-Mo2CTx MXene for the electrochemical nitrogen reduction reaction, J. Colloid Interface Sci. 605 (2022) 897–905. https://doi.org/10.1016/j.jcis.2021.07.083.

[27] Y. Gao, Y. Cao, H. Zhuo, X. Sun, Y. Gu, et al., Mo2TiC2 MXene: A Promising Catalyst for Electrocatalytic Ammonia Synthesis, Catal. Today. 339 (2020) 120–126. https://doi.org/10.1016/j.cattod.2018.12.029.

[28] Y. Wang, X. Hu, H. Song, Y. Cai, Z. Li, et al., Oxygen vacancies in actiniae-like Nb2O5/Nb2C MXene heterojunction boosting visible

light photocatalytic NO removal, Appl. Catal. B. 299 (2021) 120677. https://doi.org/10.1016/j.apcatb.2021.120677.
[29] T. Su, R. Peng, Z.D. Hood, M. Naguib, I.N. Ivanov, et al., One-Step Synthesis of Nb2O5/C/Nb2C (MXene) Composites and Their Use as Photocatalysts for Hydrogen Evolution, ChemSunChem. 11 (2018) 688–699. https://doi.org/10.1002/cssc.201702317.
[30] D. Zu, H. Song, Y. Wang, Z. Chao, Z. Li, et al., One-pot in-situ hydrothermal synthesis of CdS/Nb2O5/Nb2C heterojunction for enhanced visible-light-driven photodegradation, Appl. Catal. B. 277 (2020) 119140. https://doi.org/10.1016/j.apcatb.2020.119140.
[31] A. Sherryna, M. Tahir, Role of Ti3C2 MXene as Prominent Schottky Barriers in Driving Hydrogen Production through Photoinduced Water Splitting: A Comprehensive Review, ACS Appl. Energy Mater. 4 (2021) 11982–12006. https://doi.org/10.1021/acsaem.1c02241.
[32] S.D. Chakraborty, P. Bhattacharya, T. Mishra, Recent advances in 2D MXene-based heterostructured photocatalytic materials, Sustainable Material Solutions for Solar Energy Technologies, Processing Techniques and Applications, Solar Cell Engineering, Elsevier. (2021) 329–362. https://doi.org/10.1016/B978-0-12-821592-0.00005-4.
[33] P. Gnanasekar, J. Kulandaivel, Two-Dimensional Materials for Renewable Energy Devices, Encyclopedia of Applied Physics, Wiley-VCH Verlag GmbH & Co. KGaA (Ed.). (2021). https://doi.org/10.1002/3527600434.eap957.
[34] L. Biswal, S. Nayak, K. Parida, Recent progress on strategies for the preparation of 2D/2D MXene/g-C3N4 nanocomposites for photocatalytic energy and environmental applications, Catal. Sci. Technol. 11 (2021) 1222–1248. https://doi.org/10.1039/D0CY02156C.
[35] S.B. Ambade, R.B. Ambade, W. Eom, S.H. Noh, S.H. Kim, T.H. Han, 2D Ti3C2 MXene/WO3 Hybrid Architectures for High-Rate Supercapacitors, Adv. Mater. Interfaces. 5 (2018) 1801361. https://doi.org/10.1002/admi.201801361.
[36] X. Feng, Z. Yu, Y. Sun, M. Shan, R. Long, X. Li, 3D MXene/Ag2S material as Schottky junction catalyst with stable and enhanced photocatalytic activity and photocorrosion resistance, Sep. Purif. Technol. 266 (2021) 118606. https://doi.org/10.1016/j.seppur.2021.118606.
[37] L. Biswal, R. Mohanty, S. Nayak, K. Parida, Review on MXene/TiO2 nanohybrids for photocatalytic hydrogen production and pollutant degradations, J. Environ. Chem. Eng. 10 (2022) 107211. https://doi.org/10.1016/j.jece.2022.107211.
[38] V.-H. Nguyen, B.-S. Nguyen, C. Hu, C.C. Nguyen, D.L.T. Nguyen, et al., Novel Architecture Titanium Carbide (Ti3C2Tx) MXene Cocatalysts toward Photocatalytic Hydrogen Production: A Mini-Review, Nanomaterials. 10 (2020) 602. https://doi.org/10.3390/nano10040602.
[39] Y. Li, Y. Liu, T. Zheng, S.-i. Ssaki, H. Tamiaki, X.-F. Wang, Chlorophyll derivative sensitized monolayer Ti3C2Tx MXene nanosheets for photocatalytic hydrogen evolution, J. Photochem. Photobiol. A. 427 (2022) 113792. https://doi.org/10.1016/j.jphotochem.2022.113792.
[40] M. Tahir, A. Sherryna, R. Mansoor, A.A. Khan, S. Tasleem, B. Tahir, Titanium Carbide MXene Nanostructures as Catalysts and Cocatalysts for Photocatalytic Fuel Production: A Review, ACS Appl. Nano Mater. 5 (2022) 18–54. https://doi.org/10.1021/acsanm.1c03112.
[41] K.R.G. Lim, A.D. Handoko, S.K. Nemani, B. Wyatt, H.-Y. Jiang, et al., Rational Design of Two-Dimensional Transition Metal Carbide/Nitride (MXene) Hybrids and Nanocomposites for Catalytic Energy Storage and Conversion, ACS Nano. 14 (2020) 10834–10864. https://doi.org/10.1021/acsnano.0c05482.
[42] G. Gao, A.P. O'Mullane, A. Du, 2D MXenes: A New Family of Promising Catalysts for the Hydrogen Evolution Reaction, ACS Catal. 7 (2017) 494–500. https://doi.org/10.1021/acscatal.6b02754.
[43] X. Yang, D. Singh, R. Ahuja, Recent Advancements and Future Prospects in Ultrathin 2D Semiconductor-Based Photocatalysts for Water Splitting, Catalysts. 10 (2020) 1111. https://doi.org/10.3390/catal10101111.
[44] F. Zhang, S.S. Wong, Controlled Synthesis of Semiconducting Metal Sulfide Nanowires, Chem. Mater. 21 (2009) 4541–4554. https://doi.org/10.1021/cm901492f.
[45] A. Akhoondi, M. Aghaziarati, N. Khandan, Production of highly pure iron disulfide nanoparticles using hydrothermal synthesis method, Appl. Nanosci. 3 (2013) 417–422. https://doi.org/10.1007/s13204-012-0153-1.
[46] S. Iqbal, A. Bahadur, S. Anwer, S. Ali, A. Saeed, et al., Shape and phase-controlled synthesis of specially designed 2D morphologies of l-cysteine surface capped covellite (CuS) and chalcocite (Cu2S) with excellent photocatalytic properties in the visible spectrum, Appl. Surf. Sci. 526 (2020) 146691. https://doi.org/10.1016/j.apsusc.2020.146691.
[47] H. Wang, Y. Wu, T. Xiao, X. Yuan, G. Zeng, et al., Formation of quasi-core-shell In2S3/anatase TiO2@metallic Ti3C2Tx hybrids with favorable charge transfer channels for excellent visible-light-photocatalytic performance, Appl. Catal. B. 233 (2018) 213–225. https://doi.org/10.1016/j.apcatb.2018.04.012.
[48] S. Guo, L. Yang, Y. Zhang, Z. Huang, X. Ren, et al., Enhanced hydrogen evolution via interlaced Ni3S2/MoS2 heterojunction photocatalysts with efficient interfacial contact and broadband absorption, J. Alloys Compd. 749 (2018) 473–480. https://doi.org/10.1016/j.jallcom.2018.03.329.
[49] C.-H. Lai, M.-Y. Lu, L.-J. Chen, Metal sulfide nanostructures: synthesis, properties and applications in energy conversion and storage, J. Mater. Chem. 22 (2012) 19–30. https://doi.org/10.1039/C1JM13879K.
[50] H. Kisch, Semiconductor Photocatalysis for Chemoselective Radical Coupling Reactions, Acc. Chem. Res. 50 (2017) 1002–1010. https://doi.org/10.1021/acs.accounts.7b00023.
[51] S.-C. Zhu, S. Li, B. Tang, H. Liang, B.-J. Liu, et al., MXene-motivated accelerated charge transfer over TMCs quantum dots for solar-powered photoreduction catalysis, J. Catal. 404 (2021) 56–66. https://doi.org/10.1016/j.jcat.2021.09.001.
[52] S. Shanmugaratnam, S. Rasalingam, Transition Metal Chalcogenide (TMC) Nanocomposites for Environmental Remediation Application over Extended Solar Irradiation, Nanocatalysts, IntechOpen. (2019). https://doi.org/10.5772/intechopen.83628.
[53] T. Heine, Transition Metal Chalcogenides: Ultrathin Inorganic Materials with Tunable Electronic Properties, Acc. Chem. Res. 48 (2015) 65–72. https://doi.org/10.1021/ar500277z.
[54] C. Prasad, X. Yang, Q. Liu, H. Tang, A. Rammohan, et al., Recent advances in MXenes supported semiconductors based photocatalysts: Properties, synthesis and photocatalytic applications, J. Ind. Eng. Chem. 85 (2020) 1–33. https://doi.org/10.1016/j.jiec.2019.12.003.
[55] W.-K. Jo, T.S. Natarajan, Influence of TiO2 morphology on the photocatalytic efficiency of direct Z-scheme g-C3N4/TiO2 photocatalysts for isoniazid degradation, Chem. Eng. J. 281 (2015) 549–565. https://doi.org/10.1016/j.cej.2015.06.120.
[56] A. Sherryna, M. Tahir, Role of surface morphology and terminating groups in titanium carbide MXenes (Ti3C2Tx) cocatalysts with engineering aspects for modulating solar hydrogen production: A critical review, Chem. Eng. J. 433 (2022) 134573. https://doi.org/10.1016/j.cej.2022.134573.
[57] S. Kahng, H. Yoo, J.H. Kim, Recent advances in earth-abundant photocatalyst materials for solar H2 production, Adv. Powder Technol. 31 (2020) 11–28. https://doi.org/10.1016/j.apt.2019.08.035.
[58] A. Kudo, Y. Miseki, Heterogeneous photocatalyst materials for water splitting, Chem. Soc. Rev. 38 (2009) 253–278. https://doi.org/10.1039/B800489G.
[59] X. Liu, P. Wang, X. Liang, Q. Zhang, Z. Wang, et al., Research progress and surface/interfacial regulation methods for electrophotocatalytic hydrogen production from water splitting,

Mater Today Energy. 18 (2020) 100524. https://doi.org/10.1016/j.mtener.2020.100524.
[60] V. Kumaravel, M. Danyal Imam, A. Badreldin, R.K. Chava, J.Y. Do, et al., Photocatalytic Hydrogen Production: Role of Sacrificial Reagents on the Activity of Oxide, Carbon, and Sulfide Catalysts, Catalysts. 9 (2019) 276. https://doi.org/10.3390/catal9030276.
[61] M. Kang, V. Kumaravel, Photocatalytic Hydrogen Evolution, Catalysts. (2020). https://doi.org/10.3390/books978-3-03936-311-7.
[62] Y. Li, J. Wang, S. Peng, G. Lu, S. Li, Photocatalytic hydrogen generation in the presence of glucose over ZnS-coated ZnIn2S4 under visible light irradiation, Int. J. Hyrog. Energy. 35 (2010) 7116–7126. https://doi.org/10.1016/j.ijhydene.2010.02.017.
[63] M. Naguib, O. Mashtalir, J. Carle, V. Presser, J. Lu, et al., Two-Dimensional Transition Metal Carbides, ACS Nano. 6 (2012) 1322–1331. https://doi.org/10.1021/nn204153h.
[64] Y.L. Du, Z.M. Sun, H. Hashimoto, M.W. Barsoum, Electron correlation effects in the MAX phase Cr2AlC from first-principles, J. Appl. Phys. 109 (2011) 063707. https://doi.org/10.1063/1.3562145.
[65] D. Music, Z. Sun, J.M. Schneider, Electronic structure of Sc2AC (A=Al, Ga, In, Tl), Solid State Commun. 133 (2005) 381–383. https://doi.org/10.1016/j.ssc.2004.11.034.
[66] P. Simon, Two-Dimensional MXene with Controlled Interlayer Spacing for Electrochemical Energy Storage, ACS Nano. 11 (2017) 2393–2396. https://doi.org/10.1021/acsnano.7b01108.
[67] D. Magne, V. Mauchamp, S. Célérier, P. Chartier, T. Cabioc'h, Site-projected electronic structure of two-dimensional Ti3C2 MXene: the role of the surface functionalization groups, Phys. Chem. Chem. Phys. 18 (2016) 30946–30953. https://doi.org/10.1039/C6CP05985F.
[68] M.A. Iqbal, S.I. Ali, F. Amin, A. Tariq, M.Z. Iqbal, S. Rizwan, La- and Mn-Codoped Bismuth Ferrite/Ti3C2 MXene Composites for Efficient Photocatalytic Degradation of Congo Red Dye, ACS Omega. 4 (2019) 8661–8668. https://doi.org/10.1021/acsomega.9b00493.
[69] L. Wang, W. Tao, L. Yuan, Z. Liu, O. Huang, et al., Rational control of the interlayer space inside two-dimensional titanium carbides for highly efficient uranium removal and imprisonment, Chem. Commun. 53 (2017) 12084–12087. https://doi.org/10.1039/C7CC06740B.
[70] L. Li, F. Wang, J. Zhu, W. Wu, The facile synthesis of layered Ti2C MXene/carbon nanotube composite paper with enhanced electrochemical properties, Dalton Trans. 46 (2017) 14880–14887. https://doi.org/10.1039/C7DT02688A.
[71] S. Ahmad, I. Ashraf, M.A. Mansoor, S. Rizwan, M. Iqbal, An Overview of Recent Advances in the Synthesis and Applications of the Transition Metal Carbide Nanomaterials, Nanomaterials. 11 (2021) 776. https://doi.org/10.3390/nano11030776.
[72] S. Biswas, P.S. Alegaonkar, MXene: Evolutions in Chemical Synthesis and Recent Advances in Applications, Surfaces. 5 (2022) 1–34. https://doi.org/10.3390/surfaces5010001.
[73] G. Li, L. Tan, Y. Zhang, B. Wu, L. Li, Highly Efficiently Delaminated Single-Layered MXene Nanosheets with Large Lateral Size, Langmuir. 33 (2017) 9000–9006. https://doi.org/10.1021/acs.langmuir.7b01339.
[74] C. Kai, F. Zhang, C. Kong, W. Cai, Progress in photocatalysis of new two-dimensional layered materials MXenes, Rev. Roum. Chim. 12 (2020) 1079–1091. https://doi.org/10.33224/rrch.2020.65.12.03.
[75] C. Peng, T. Zhou, P. Wei, H. Ai, B. Zhou, et al., Regulation of the rutile/anatase TiO2 phase junction in-situ grown on –OH terminated Ti3C2Tx (MXene) towards remarkably enhanced photocatalytic hydrogen evolution, Chem. Eng. J. 439 (2022) 135685. https://doi.org/10.1016/j.cej.2022.135685.
[76] H. Zong, R. Qi, K. Yu, Z. Zhu, Ultrathin Ti2NTx MXene-wrapped MOF-derived CoP frameworks towards hydrogen evolution and water oxidation, Electrochim. Acta. 393 (2021) 139068. https://doi.org/10.1016/j.electacta.2021.139068.
[77] K. Huang, C. Li, X. Zhang, L. Wang, W. Wang, X. Meng, Self-assembly synthesis of phosphorus-doped tubular g-C3N4/Ti3C2 MXene Schottky junction for boosting photocatalytic hydrogen evolution, Green Energy Environ. 8 (2023) 233–245. https://doi.org/10.1016/j.gee.2021.03.011.
[78] M. Zhang, J. Qin, S. Rajendran, X. Zhang, R. Liu, Heterostructured d-Ti3C2/TiO2/g-C3N4 Nanocomposites with Enhanced Visible-Light Photocatalytic Hydrogen Production Activity, ChemSunChem. 11 (2018) 4226–4236. https://doi.org/10.1002/cssc.201802284.
[79] M. Mozafari, M. Soroush, Surface functionalization of MXenes, Mater. Adv. 2 (2021) 7277–7307. https://doi.org/10.1039/D1MA00625H.
[80] J.L. Hart, K. Hantanasirisakul, A.C. Lang, B. Anasori, D. Pinto, et al., Control of MXenes' electronic properties through termination and intercalation, Nat. Commun. 10 (2019) 522. https://doi.org/10.1038/s41467-018-08169-8.
[81] G. Huang, C.-H. Lu, H.-H. Yang, Novel Nanomaterials for Biomedical, Environmental and Energy Applications, Elsevier. (2019) 89–109. https://doi.org/10.1016/B978-0-12-814497-8.00003-5.
[82] B.P. Kafle, Introduction to nanomaterials and application of UV–Visible spectroscopy for their characterization, Chemical Analysis and Material Characterization by Spectrophotometry, Elsevier. (2020) 147–198. https://doi.org/10.1016/B978-0-12-814866-2.00006-3.
[83] A. Akhoondi, M. Ziarati, N. Khandan, Hydrothermal Production of Highly Pure Nano Pyrite in a Stirred Reactor, Iran. J. Chem. Chem. Eng. 33 (2014) 15–19. https://doi.org/10.30492/IJCCE.2014.7189.
[84] Y.X. Gan, A.H. Jayatissa, Z. Yu, X. Chen, M. Li, Hydrothermal Synthesis of Nanomaterials, J. Nanomater. 2020 (2020) 8917013. https://doi.org/10.1155/2020/8917013.
[85] A.D. Li, W.C. Liu, Optical properties of ferroelectric nanocrystal/polymer composites, Physical Properties and Applications of Polymer Nanocomposites, Woodhead Publishing. (2010) 108–158. https://doi.org/10.1533/9780857090249.1.108.
[86] N. Asim, S. Ahmadi, M.A. Alghoul, F.Y. Hammadi, K. Saeedfar, K. Sopian, Research and Development Aspects on Chemical Preparation Techniques of Photoanodes for Dye Sensitized Solar Cells, Int. J. Photoenergy. 2014 (2014) 518156. https://doi.org/10.1155/2014/518156.
[87] G. Zou, H. Li, Y. Zhang, K. Xiong, Y. Qian, Solvothermal/hydrothermal route to semiconductor nanowires, Nanotechnology. 17 (2006) S313. https://doi.org/10.1088/0957-4484/17/11/S14.
[88] L. Tie, S. Yang, C. Yu, H. Chen, Y. Liu, et al., In situ decoration of ZnS nanoparticles with Ti3C2 MXene nanosheets for efficient photocatalytic hydrogen evolution, J. Colloid Interf. Sci. 545 (2019) 63–70. https://doi.org/10.1016/j.jcis.2019.03.014.
[89] A. Akhoondi, A.I. Osman, A. Alizadeh Eslami, Direct catalytic production of dimethyl ether from CO and CO2: A review, Synth. Sinter. 1 (2021) 105–120. https://doi.org/10.53063/synsint.2021.1229.
[90] C. Su, B.-Y. Hong, C.-M. Tseng, Sol–gel preparation and photocatalysis of titanium dioxide, Catal. Today. 96 (2004) 119–126. https://doi.org/10.1016/j.cattod.2004.06.132.
[91] E.M. Modon, A.G. Plăiașu, Advantages and Disadvantages of Chemical Methods in the Elaboration of Nanomaterials, The Annals of "Dunarea de Jos" University of Galati. Fascicle IX, Metall. Mater. Sci. 43 (2020) 53–60. https://doi.org/10.35219/mms.2020.1.08.
[92] H. Xiao, Z. Chen, K. Sun, C. Yan, J. Xiao, et al., Sol-gel solution-processed Cu2SrSnS4 thin films for solar energy harvesting, Thin Solid Films. 697 (2020) 137828. https://doi.org/10.1016/j.tsf.2020.137828.
[93] D. Tetzlaff, C. Simon, D.S. Achilleos, M. Smialkowski, K.j. Puring, et al., FexNi9−xS8 (x = 3–6) as potential photocatalysts for solar-driven hydrogen production?, Faraday Discuss. 215 (2019) 216–226. https://doi.org/10.1039/C8FD00173A.
[94] H. Xu, B.W. Zeiger, K.S. Suslick, Sonochemical synthesis of nanomaterials, Chem. Soc. Rev. 42 (2013) 2555–2567. https://doi.org/10.1039/C2CS35282F.

[95] J. Ran, G. Gao, F.-T. Li, T.-Y. Ma, A. Du, S.-Z. Qiao, Ti3C2 MXene co-catalyst on metal sulfide photo-absorbers for enhanced visible-light photocatalytic hydrogen production, Nat. Commun. 8 (2017) 13907. https://doi.org/10.1038/ncomms13907.

[96] J.-Y. Li, Y.-H. Li, F. Zhang, Z.-R. Tang, Y.-J. Xu, Visible-light-driven integrated organic synthesis and hydrogen evolution over 1D/2D CdS-Ti3C2Tx MXene composites, Appl. Catal. B. 269 (2020) 118783. https://doi.org/10.1016/j.apcatb.2020.118783.

[97] R. Xiao, C. Zhao, Z. Zou, Z. Chen, L. Tian, et al., In situ fabrication of 1D CdS nanorod/2D Ti3C2 MXene nanosheet Schottky heterojunction toward enhanced photocatalytic hydrogen evolution, Appl. Catal. B. 268 (2020) 118382. https://doi.org/10.1016/j.apcatb.2019.118382.

[98] X. Chen, Y. Guo, R. Bian, Y. Ji, X. Wang, et al., Titanium carbide MXenes coupled with cadmium sulfide nanosheets as two-dimensional/two-dimensional heterostructures for photocatalytic hydrogen production, J. Colloid Interface Sci. 613 (2022) 644–651. https://doi.org/10.1016/j.jcis.2022.01.079.

[99] J. Yin, F. Zhan, T. Jiao, W. Wang, G. Zhang, et al., Facile preparation of self-assembled MXene@Au@CdS nanocomposite with enhanced photocatalytic hydrogen production activity, Sci. China Mater. 63 (2020) 2228–2238. https://doi.org/10.1007/s40843-020-1299-4.

[100] Y. Yang, D. Zhang, Q. Xiang, Plasma-modified Ti3C2Tx/CdS hybrids with oxygen-containing groups for high-efficiency photocatalytic hydrogen production, Nanoscale. 11 (2019) 18797–18805. https://doi.org/10.1039/C9NR07242J.

[101] Z. Ai, K. Zhang, B. Chang, Y. Shao, L. Zhang, et al., Construction of CdS@Ti3C2@CoO hierarchical tandem p-n heterojunction for boosting photocatalytic hydrogen production in pure water, Chem. Eng. J. 383 (2020) 123130. https://doi.org/10.1016/j.cej.2019.123130.

[102] S. Jin, Z. Shi, H. Jing, L. Wang, Q. Hu, et al., Mo2C-MXene/CdS Heterostructures as Visible-Light Photocatalysts with an Ultrahigh Hydrogen Production Rate, ACS Appl. Energy Mater. 4 (2021) 12754–12766. https://doi.org/10.1021/acsaem.1c02456.

[103] W. Wang, Z.D. Hood, X. Zhang, I.N. Ivanov, Z. Bao, et al., Construction of 2D BiVO4−CdS−Ti3C2Tx Heterostructures for Enhanced Photo-redox Activities, ChemCatChem. 12 (2020) 3496–3503. https://doi.org/10.1002/cctc.202000448.

[104] M. Ding, R. Xiao, C. Zhao, D. Bukhvalov, Z. Chen, et al., Evidencing Interfacial Charge Transfer in 2D CdS/2D MXene Schottky Heterojunctions toward High-Efficiency Photocatalytic Hydrogen Production, Sol. RRL. 5 (2021) 2000414. https://doi.org/10.1002/solr.202000414.

[105] X. Liu, Q. Liu, C. Chen, Ultrasonic oscillation synthesized ZnS nanoparticles/layered MXene sheet with outstanding photocatalytic activity under visible light, Vacuum. 183 (2021) 109834. https://doi.org/10.1016/j.vacuum.2020.109834.

[106] Y. Li, Z. Yin, G. Ji, Z. Liang, Y. Xue, et al., 2D/2D/2D heterojunction of Ti3C2 MXene/MoS2 nanosheets/TiO2 nanosheets with exposed (001) facets toward enhanced photocatalytic hydrogen production activity, Appl. Catal. B. 246 (2019) 12–20. https://doi.org/10.1016/j.apcatb.2019.01.051.

[107] Y. Li, S. Yang, Z. Liang, Y. Xue, H. Cui, J. Tian, 1T-MoS2 nanopatch/Ti3C2 MXene/TiO2 nanosheet hybrids for efficient photocatalytic hydrogen evolution, Mater. Chem. Front. 3 (2019) 2673–2680. https://doi.org/10.1039/C9QM00608G.

[108] Y. Li, L. Ding, Z. Liang, Y. Xue, H. Cui, J. Tian, Synergetic effect of defects rich MoS2 and Ti3C2 MXene as cocatalysts for enhanced photocatalytic H2 production activity of TiO2, Chem. Eng. J. 383 (2020) 123178. https://doi.org/10.1016/j.cej.2019.123178.

[109] J. Zhang, C. Xing, F. Shi, MoS2/Ti3C2 heterostructure for efficient visible-light photocatalytic hydrogen generation, Int. J. Hydrog. Energy. 45 (2020) 6291–6301. https://doi.org/10.1016/j.ijhydene.2019.12.109.

[110] Z. Yao, H. Sun, H. Sui, X. Liu, 2D/2D Heterojunction of R-scheme Ti3C2 MXene/MoS2 Nanosheets for Enhanced Photocatalytic Performance, Nanoscale Res. Lett. 15 (2020) 78. https://doi.org/10.1186/s11671-020-03314-z.

[111] Y. Li, L. Ding, S. Yin, Z. Liang, Y. Xue, et al., Photocatalytic H2 Evolution on TiO2 Assembled with Ti3C2 MXene and Metallic 1T-WS2 as Co-catalysts, Nano-Micro Lett. 12 (2020) 6. https://doi.org/10.1007/s40820-019-0339-0.

[112] K. Huang, C. Li, X. Meng, In-situ construction of ternary Ti3C2 MXene@TiO2/ZnIn2S4 composites for highly efficient photocatalytic hydrogen evolution, J. Colloid Interface Sci. 580 (2020) 669–680. https://doi.org/10.1016/j.jcis.2020.07.044.

[113] G. Zuo, Y. Wang, W.L. Teo, M. Xie, Y. Guo, et al., Ultrathin ZnIn2S4 Nanosheets Anchored on Ti3C2TX MXene for Photocatalytic H2 Evolution, Angew. Chem. Int. 132 (2020) 11383–11388. https://doi.org/10.1002/ange.202002136.

[114] H. Wang, Y. Sun, Y. Wu, W. Tu, S. Wu, et al., Electrical promotion of spatially photoinduced charge separation via interfacial-built-in quasi-alloying effect in hierarchical Zn2In2S5/Ti3C2(O, OH)x hybrids toward efficient photocatalytic hydrogen evolution and environmental remediation, Appl. Catal. B. 245 (2019) 290–301. https://doi.org/10.1016/j.apcatb.2018.12.051.

[115] M. Ou, J. Li, Y. Chen, S. Wan, S. Zhao, et al., Formation of noble-metal-free 2D/2D ZnmIn2Sm+3 (m = 1, 2, 3)/MXene Schottky heterojunction as an efficient photocatalyst for hydrogen evolution, Chem. Eng. J. 424 (2021) 130170. https://doi.org/10.1016/j.cej.2021.130170.

[116] T. Su, C. Men, L. Chen, B. Chu, X. Luo, et al., Sulfur Vacancy and Ti3C2Tx Cocatalyst Synergistically Boosting Interfacial Charge Transfer in 2D/2D Ti3C2Tx/ZnIn2S4 Heterostructure for Enhanced Photocatalytic Hydrogen Evolution, Adv. Sci. 9 (2022) 2103715. https://doi.org/10.1002/advs.202103715.

[117] L. Pan, H. Mei, H. Liu, H. Pan, X. Zhao, et al., High-efficiency carrier separation heterostructure improve the photocatalytic hydrogen production of sulfide, J. Alloys Compd. 817 (2020) 153242. https://doi.org/10.1016/j.jallcom.2019.153242.

[118] B. Cao, S. Wan, Y. Wang, H. Guo, M. Ou, Q. Zhong, Highly-efficient visible-light-driven photocatalytic H2 evolution integrated with microplastic degradation over MXene/ZnxCd1-xS photocatalyst, J. Colloid Interface Sci. 605 (2022) 311–319. https://doi.org/10.1016/j.jcis.2021.07.113.

[119] G. Zeng, Y. Cao, Y. Wu, H. Yuan, B. Zhang, et al., Cd0.5Zn0.5S/Ti3C2 MXene as a Schottky catalyst for highly efficient photocatalytic hydrogen evolution in seawater, Appl. Mater. Today. 22 (2021) 100926. https://doi.org/10.1016/j.apmt.2020.100926.

[120] S. Zheng, S. Peng, Z. Wang, J. Huang, X. Luo, et al., Schottky-structured 0D/2D composites via electrostatic self-assembly for efficient photocatalytic hydrogen evolution, Ceram. Int. 47 (2021) 28304–28311. https://doi.org/10.1016/j.ceramint.2021.06.247.

[121] L. Cheng, Q. Chen, J. Li, H. Liu, Boosting the photocatalytic activity of CdLa2S4 for hydrogen production using Ti3C2 MXene as a co-catalyst, Appl. Catal. B. 267 (2020) 118379. https://doi.org/10.1016/j.apcatb.2019.118379.

[122] W. Yang, G. Ma, Y. Fu, K. Peng, H. Yang, et al., Rationally designed Ti3C2 MXene@TiO2/CuInS2 Schottky/S-scheme integrated heterojunction for enhanced photocatalytic hydrogen evolution, Chem. Eng. J. 429 (2022) 132381. https://doi.org/10.1016/j.cej.2021.132381.

[123] J.-H. Zhao, L.-W. Liu, K. Li, T. Li, F.-T. Liu, Conductive Ti3C2 and MOF-derived CoSx boosting the photocatalytic hydrogen production activity of TiO2, CrystEngComm. 21 (2019) 2416–2421. https://doi.org/10.1039/C8CE02050G.

[124] Y. Xie, M.M. Rahman, S. Kareem, H. Dong, F. Qiao, et al., Facile synthesis of CuS/MXene nanocomposites for efficient photocatalytic hydrogen generation, CrystEngComm. 22 (2020) 2060–2066. https://doi.org/10.1039/D0CE00104J.

[125] Y.-J. Yuan, D. Chen, Z.-T. Yu, Z.-G. Zou, Cadmium sulfide-based nanomaterials for photocatalytic hydrogen production, J. Mater. Chem. A. 6 (2018) 11606–11630. https://doi.org/10.1039/C8TA00671G.

[126] G.-J. Lee, J.J. Wu, Recent developments in ZnS photocatalysts from synthesis to photocatalytic applications — A review, Powder Technol. 318 (2017) 8–22. https://doi.org/10.1016/j.powtec.2017.05.022.

[127] B. Archana, N. Kottam, S. Nayak, K.B. Chandrasekhar, M.B. Sreedhara, Superior Photocatalytic Hydrogen Evolution Performances of WS2 over MoS2 Integrated with CdS Nanorods, J. Phys. Chem. C. 124 (2020) 14485–14495. https://doi.org/10.1021/acs.jpcc.0c03411.

[128] Q. Wang, J. Li, Y. Bai, J. Lian, H. Huang, et al., Photochemical preparation of Cd/CdS photocatalysts and their efficient photocatalytic hydrogen production under visible light irradiation, Green Chem. 16 (2014) 2728–2735. https://doi.org/10.1039/C3GC42466A.

[129] S. Tso, W.-S. Li, B.-H. Wu, L.-J. Chen, Enhanced H2 production in water splitting with CdS-ZnO core-shell nanowires, Nano Energy. 43 (2018) 270–277. https://doi.org/10.1016/j.nanoen.2017.11.048.

[130] G.-J. Lee, S. Anandan, S.J. Masten, J.J. Wu, Sonochemical Synthesis of Hollow Copper Doped Zinc Sulfide Nanostructures: Optical and Catalytic Properties for Visible Light Assisted Photosplitting of Water, Ind. Eng. Chem. Res. 53 (2014) 8766–8772. https://doi.org/10.1021/ie500663n.

[131] H. Tada, M. Mitsui, T. Kiyonaga, T. Akita, K. Tanaka, All-solid-state Z-scheme in CdS–Au–TiO2 three-component nanojunction system, Nat. Mater. 5 (2006) 782–786. https://doi.org/10.1038/nmat1734.

[132] M. Li, Z. Cui, E. Li, Silver-modified MoS2 nanosheets as a high-efficiency visible-light photocatalyst for water splitting, Ceram. Int. 45 (2019) 14449–14456. https://doi.org/10.1016/j.ceramint.2019.04.166.

[133] Q. Xiang, F. Cheng, D. Lang, Hierarchical Layered WS2/Graphene-Modified CdS Nanorods for Efficient Photocatalytic Hydrogen Evolution, ChemsunChem. 9 (2016) 996–1002. https://doi.org/10.1002/cssc.201501702.

[134] T.P. Nguyen, Q. Van Le, K.S. Choi, J.H. Oh, Y.G. Kim, et al., MoS2 Nanosheets Exfoliated by Sonication and Their Application in Organic Photovoltaic Cells, Sci. Adv. Mater. 7 (2015) 700–705. https://doi.org/10.1166/sam.2015.1891.

[135] X. Zong, J. Han, G. Ma, H. Yan, G. Wu, C. Li, Photocatalytic H2 Evolution on CdS Loaded with WS2 as Cocatalyst under Visible Light Irradiation, J. Phys. Chem. C. 115 (2011) 12202–12208. https://doi.org/10.1021/jp2006777.

[136] X. Zong, G. Wu, H. Yan, G. Ma, J. Shi, et al., Photocatalytic H2 Evolution on MoS2/CdS Catalysts under Visible Light Irradiation, J. Phys. Chem. C. 114 (2010) 1963–1968. https://doi.org/10.1021/jp904350e.

[137] Q.H. Wang, K. Kalantar-Zadeh, A. Kis, J.N. Coleman, M.S. Strano, Electronics and optoelectronics of two-dimensional transition metal dichalcogenides, Nat. Nanotech. 7 (2012) 699–712. https://doi.org/10.1038/nnano.2012.193.

[138] K.F. Mak, C. Lee, J. Hone, J. Shan, T.F. Heinz, Atomically Thin MoS2 A New Direct-Gap Semiconductor, Phys. Rev. Lett. 105 (2010) 136805. https://doi.org/10.1103/PhysRevLett.105.136805.

[139] K. Chang, X. Hai, J. Ye, Transition Metal Disulfides as Noble-Metal-Alternative Co-Catalysts for Solar Hydrogen Production, Adv. Energy. Mater. 6 (2016) 1502555. https://doi.org/10.1002/aenm.201502555.

[140] B.-J. Ng, L. K. Putri, X.Y. Kong, K.P.Y. Shak, P. Pasbakhsh, et al., Sub-2 nm Pt-decorated Zn0.5Cd0.5S nanocrystals with twin-induced homojunctions for efficient visible-light-driven photocatalytic H2 evolution, Appl. Catal. B. 224 (2018) 360–367. https://doi.org/10.1016/j.apcatb.2017.10.005.

[141] H. Abid, G. Rekhila, F.A. Ihaddadene, Y. Bessekhouad, M. Trari, Hydrogen evolution under visible light illumination on the solid solution CdxZn1-xS prepared by ultrasound-assisted route, Int. J. Hydrog. Energy. 44 (2019) 10301–10308. https://doi.org/10.1016/j.ijhydene.2019.02.231.

[142] C. Xing, Y. Zhang, W. Yan, L. Guo, Band structure-controlled solid solution of Cd1-x ZnxS photocatalyst for hydrogen production by water splitting, Int. J. Hydrog. Energy. 31 (2006) 2018–2024. https://doi.org/10.1016/j.ijhydene.2006.02.003.

[143] H. Du, K. Liang, C.-Z. Yuan, H.L. Guo, X. Zhou, et al., Bare Cd1–xZnxS ZB/WZ Heterophase Nanojunctions for Visible Light Photocatalytic Hydrogen Production with High Efficiency, ACS Appl. Mater. Interfaces. 8 (2016) 24550–24558. https://doi.org/10.1021/acsami.6b06182.

[144] R. Janani, R. Preethi V, S. Singh, A. Rani, C.-T. Chang, Hierarchical Ternary Sulfides as Effective Photocatalyst for Hydrogen Generation Through Water Splitting: A Review on the Performance of ZnIn2S4, Catalysts. 11 (2021) 277. https://doi.org/10.3390/catal11020277.

[145] J. Bai, W. Chen, R. Shen, Z. Jiang, P. Zhang, et al., Regulating interfacial morphology and charge-carrier utilization of Ti3C2 modified all-sulfide CdS/ZnIn2S4 S-scheme heterojunctions for effective photocatalytic H2 evolution, J. Mater. Sci. Technol. 112 (2022) 85–95. https://doi.org/10.1016/j.jmst.2021.11.003.

[146] Z. Ai, Y. Shao, B. Chang, B. Huang, Y. Wu, X. Hao, Effective orientation control of photogenerated carrier separation via rational design of a Ti3C2(TiO2)@CdS/MoS2 photocatalytic system, Appl. Catal. B. 242 (2019) 202–208. https://doi.org/10.1016/j.apcatb.2018.09.101.

[147] R. Chen, P. Wang, J. Chen, C. Wang, Y. Ao, Synergetic effect of MoS2 and MXene on the enhanced H2 evolution performance of CdS under visible light irradiation, App. Surf. Sci. 473 (2019) 11–19. https://doi.org/10.1016/j.apsusc.2018.12.071.